



HAL
open science

Fish shrinking, energy balance and climate change

Quentin Queiros, David J Mckenzie, Gilbert Dutto, Shaun Killen, Claire Saraux, Quentin Schull

► **To cite this version:**

Quentin Queiros, David J Mckenzie, Gilbert Dutto, Shaun Killen, Claire Saraux, et al.. Fish shrinking, energy balance and climate change. *Science of the Total Environment*, 2024, 906, pp.167310. 10.1016/j.scitotenv.2023.167310 . hal-04237380

HAL Id: hal-04237380

<https://hal.science/hal-04237380>

Submitted on 11 Oct 2023

HAL is a multi-disciplinary open access archive for the deposit and dissemination of scientific research documents, whether they are published or not. The documents may come from teaching and research institutions in France or abroad, or from public or private research centers.

L'archive ouverte pluridisciplinaire **HAL**, est destinée au dépôt et à la diffusion de documents scientifiques de niveau recherche, publiés ou non, émanant des établissements d'enseignement et de recherche français ou étrangers, des laboratoires publics ou privés.

Copyright

Fish shrinking, energy balance and climate change

Running title: Energy balance and fish shrinking

Authors: Quentin Queiros^{a,b*}, David J. McKenzie^a, Gilbert Dutto^a, Shaun Killen^c, Claire Saraux^d,
Quentin Schull^a

^aMARBEC, Univ Montpellier, IFREMER, CNRS, IRD, Montpellier, Sète, Palavas-les-Flots, France

^bDECOD (Ecosystem Dynamics and Sustainability), INRAE, Institut Agro, IFREMER, Rennes,
France

^cInstitute of Biodiversity, Animal Health and Comparative Medicine, University of Glasgow,
Graham Kerr Building, Glasgow G12 8QQ, UK

^dIPHC UMR 7178, Université de Strasbourg, CNRS, Strasbourg, France

* Corresponding author: quentin.queiros@slu.se

Keywords: size decline, energy expenditure, feeding behaviour, temperature, small pelagic
fish, respirometry, experiments

19 **Abstract**

20 A decline in size is increasingly recognised as a major response by ectothermic species to
21 global warming. Mechanisms underlying this phenomenon are poorly understood but could
22 include changes in energy balance of consumers, driven by declines in prey size coupled with
23 increased energy demands due to warming. The sardine *Sardina pilchardus* is a prime
24 example of animal shrinking, European populations of this planktivorous fish are undergoing
25 profound decreases in body condition and adult size. This is apparently a bottom-up effect
26 coincident with a shift towards increased reliance on smaller planktonic prey. We investigated
27 the hypothesis that foraging on smaller prey would lead to increased rates of energy
28 expenditure by sardines, and that such expenditures would be exacerbated by warming
29 temperature. Using group respirometry we measured rates of energy expenditure indirectly,
30 as oxygen uptake, by captive adult sardines offered food of two different sizes (0.2 or 1.2 mm
31 items) when acclimated to two temperatures (16°C or 21°C). Energy expenditure during
32 feeding on small items was tripled at 16°C and doubled at 21°C compared to large items,
33 linked to a change in foraging mode between filter feeding on small or direct capture of large.
34 This caused daily energy expenditure to increase by ~10% at 16°C and ~40% at 21°C on small
35 items, compared to large items at 16°C. These results support that declines in prey size
36 coupled with warming could influence energy allocation towards life-history traits in wild
37 populations. This bottom-up effect could partially explain the shrinking and declining
38 condition of many small pelagic fish populations and may be contributing to the shrinking of
39 other fish species throughout the marine food web. Understanding how declines in prey size
40 can couple with warming to affect consumers is a crucial element of projecting the
41 consequences for marine fauna of ongoing anthropogenic global change.

42 **1. Introduction**

43 Ongoing global warming constitutes a major threat for biodiversity, especially in marine
44 ecosystems, with some scenarios of future temperature increases reaching +5°C in 2100
45 (IPCC, 2013, 2014; Orr et al., 2005). For ectotherms such as fishes, warming results in large
46 increases in their physiological rates (Clarke & Fraser, 2004; Seebacher et al., 2015). While
47 ongoing global warming might therefore be expected to boost growth rates in ectotherms
48 (Morrongiello et al., 2019; Seebacher et al., 2015), it has in fact been correlated with a
49 progressive decline in adult body size of many fish species in the wild (e.g. in Baudron et al.,
50 2014; Gardner et al., 2011; Sheridan & Bickford, 2011, but see Audzijonyte et al., 2020). The
51 factors that contribute to this shrinking of fishes are poorly understood; it is coherent with
52 how warming might affect macroecological phenomena such as Bergmann's rule and James'
53 rule, and is associated with a significantly higher proportion of younger age classes and a
54 generalised decline in individual size-at-age in populations (Daufresne et al., 2009). Shrinking
55 of fishes may also be linked to the Temperature-Size rule (TSR), the phenomenon whereby
56 warm temperatures cause more rapid early growth of ectotherms but a decline in their final
57 adult size, when compared to conspecifics reared in a cooler regime (Atkinson, 1994). The
58 mechanisms involved in the TSR remain to be elucidated, it is observed in wild populations
59 but can also be reproduced under controlled conditions in the laboratory (Forster et al., 2012;
60 Horne et al., 2015).

61 Although there has been recent theoretical focus on whether the TSR relates to respiratory
62 physiology (Verberk et al., 2021), early work focussed upon whether changes in energy
63 budget and allocation may be a major driver of fish shrinking with warming (Gardner et al.,
64 2011; Pauly et al., 2010). The availability and quality of food resources can affect individual

65 growth rates and adult body size through energy trade-offs among growth, survival and
66 reproduction (Stearns, 1989, 1992), and such effects may be exacerbated if energy
67 requirements are increased by warming. That is, it is unlikely that temperature per se is the
68 only variable involved in the size decline in wild populations, since few exceptions to this rule
69 are spreading across years, in particular studies that investigated food resources as a driver
70 explaining the TSR (e.g. in Diamond & Kingsolver, 2010; Lee et al., 2015; Ljungström et al.,
71 2020; Millien et al., 2006).

72 Temperature and food resources are both environmental variables whose variations can
73 challenge an individual's energy balance and that can drive fish life-history traits through
74 physiological processes. Thus, while the higher physiological rates due to warming cause an
75 increase in energy demands, energy availability for marine fishes is predicted to decline due
76 to climatic stressors that affect primary production and marine animal biomass (Ariza et al.,
77 2022; Bopp et al., 2005; Daufresne et al., 2009; Lotze et al., 2019). Ocean warming can amplify
78 vertical stratification and limit nutrient mixing (Roemmich & McGowan, 1995) which causes
79 declines in plankton abundance at the base of the food web and leads to communities
80 dominated by smaller-sized species and individuals (Bopp et al., 2005, 2013; Daufresne et al.,
81 2009; Richardson & Schoeman, 2004; Ward et al., 2012).

82 The first impacts of such changes at low trophic levels could be observed on planktivorous
83 species, such as small pelagic fishes (e.g. Brosset et al., 2017; van Beveren et al., 2014). These
84 species represent about 25 % of worldwide fishery landings by weight (FAO, 2018), supporting
85 the economy of several countries (Alheit et al., 2009; Fréon et al., 2005). Fluctuations of their
86 populations can have critical economic and social consequences, as observed following the
87 collapse of the Peruvian anchovy in the early 1970s (Alheit et al., 2009; Allison et al., 2009;

88 Schwartzlose et al., 1999). Population fluctuations of small pelagics are being exacerbated by
89 ongoing global change (Brochier et al., 2013; Shannon et al., 2009), so these species represent
90 key models to evaluate energetic mechanisms underlying shrinking of adult fish size.

91 In fact, small pelagic planktivorous fishes in the Mediterranean Sea are a major example of
92 shrinking (Albo-Puigserver et al., 2021; Brosset et al., 2017). There is an ongoing and profound
93 decrease in individual body size and condition of sardine (*Sardina pilchardus*) and anchovy
94 (*Engraulis encrasicolus*), which appears to be a consequence of bottom-up control mediated
95 by changes in plankton composition and abundance (Brosset et al., 2016; Saraux et al., 2019).
96 This was associated with a major regime change in the mid-2000s, with shifts of nutrient
97 inputs, water mixing and plankton production (Feuilloley et al., 2020). Since 2008, these
98 species' diet has shifted progressively from large prey (> 1 mm, especially cladocerans) to
99 increased reliance on smaller prey (< 1 mm, especially copepods), which indicates changes in
100 the plankton community towards smaller species (Brosset et al., 2016). Smaller zooplankton
101 can be less nutritious (Zarubin et al., 2014), so a decline in zooplankton size could entrain a
102 decrease in rates of energy acquisition by their predators. Identifying a clear mechanistic link
103 between a decrease in plankton size and fish growth, and ultimately population dynamics, is
104 crucial since fish shrinking is spreading to new ecosystems and species (see Bensebaini et al.,
105 2022; Véron et al., 2020).

106 Challenges to energy balance when prey become smaller could be further exacerbated in
107 fishes if prey size also influences foraging behaviour. Here, the sardine is also an interesting
108 model species. Sardines spontaneously modify their feeding behaviour according to the size
109 of their prey, using diffuse filter-feeding when prey is small but direct capture when prey is
110 large (Garrido et al., 2007, 2008). A recent long-term experiment on captive sardines showed

111 that, for the same food ration, a reduction in food size could significantly impair growth and
112 body condition (Queiros et al., 2019). Sardines filter feeding on small particles had to consume
113 twice as much as those capturing large particles to achieve the same growth and body
114 condition (Queiros et al., 2019). We suspected that the two foraging modes had different
115 energetic costs for the same degree of resource acquisition, with costs being higher for
116 sustained aerobic swimming during filter-feeding compared to brief bursts of swimming to
117 capture prey (Costalago & Palomera, 2014; Queiros et al., 2019). At the same time, food
118 availability could be highly significant in the wild, filtration could be effective in very rich areas
119 such as upwellings whereas particulate feeding might be more advantageous in areas with
120 lower prey density (Costalago et al., 2015).

121 The current study focused on this complex predator-prey interaction in a captive population
122 of adult sardines. We investigated the hypothesis that foraging on smaller prey would lead to
123 increased rates of energy expenditure by sardines, and that these energy requirements would
124 be exacerbated with warming temperature. To assess the energetic consequences of feeding
125 sardines on prey of different sizes and at different abundances, we used group respirometry
126 to measure rates of oxygen uptake and provided prey as commercial pellets of two different
127 sizes at a range of ration levels. We compared animals acclimated to two temperatures within
128 the species' thermal range, either a cool 16°C or warm 21°C. Thus, the effects on oxygen
129 consumption of particle size and temperature were investigated according to 5 scenarios: (1)
130 change from large to small particles at cool temperature; (2) change from large to small
131 particles at warm temperature; (3) rise in temperature with fish fed on large particles; (4) rise
132 in temperature with fish fed on small particles, and (5) change from large to small particles
133 while also increasing temperature. To that end, we focussed on overall daily energetic costs

134 but also a careful comparison of energetic costs incurred during and after feeding for each
135 scenario.

136

137 **2. Material and methods**

138 **2.1. Animal capture and husbandry**

139 Sardines were captured by commercial purse-seiner and transferred to the IFREMER Palavas-
140 les-Flots research station, with the same fishing and husbandry procedures as described tailed
141 in Queiros et al. (2019). Over the first week, sardines were acclimated to tanks and weaned
142 onto commercial aquaculture pellets. They were fed with a mixture of *Artemia* nauplii and
143 commercial aquaculture pellets (mix of 0.2 and 1.2 mm diameter), with increasing
144 proportions of pellets and decreasing proportions of *Artemia* throughout the week,
145 concluding exclusively with pellets. After 2-3 weeks, sardines were transferred into indoor
146 1m³ holding tanks, until experimentation. Water temperature was not set during this period
147 but followed natural fluctuations from 15 to 20°C (SST at the time of capture was 14°C).

148 **2.2. Experimental design**

149 Eighty sardines were distributed among 8 experimental tanks in groups of 10 animals (volume
150 50 L), to ensure similar distributions of body mass and condition among tanks (Fig. S1), and
151 fish densities comparable to those of Queiros et al. (2019). Fish were acclimated to the new
152 tanks while temperature was gradually changed from 19°C to either 16°C or 21°C over one
153 week. Before the experiments began, fish were fed with commercial pellets twice a day, a mix
154 of 0.2 and 1.2 mm to avoid preference bias for pellet size. These eighty sardines were used

155 for both experiments 1 and 2, described below, and these two experiments were performed
156 sequentially in the same setup.

157 The tanks were modified to function as open automated respirometers (McKenzie et al., 2007,
158 2012; Queiros et al., 2021) using the principles of cyclical intermittent stopped flow
159 (Steffensen, 1989), as described below. Four tanks were held at each of the two
160 temperatures, each set of four was supplied by water from a single reservoir where water
161 temperature was regulated by an Ice 3000 (Aquavie) at 16°C or by a Red Line heater (Zodiac)
162 at 21°C. Water in the reservoir was vigorously aerated, to maintain oxygen saturation and
163 ensure thorough mixing. Water was delivered to tank respirometers by submersible pumps
164 (Eheim 3400); within each respirometer the water was also gently but thoroughly mixed by a
165 submersible pump (Newa Maxi 500) to avoid any thermal or oxygen gradients (see
166 Supplementary Material and Fig. S2).

167 All respirometers were exposed to a 12L:12D photoperiod (L: light, D: darkness) with a natural
168 sunlight spectrum and 30 minute progressive dawns and sunsets. Individual total length and
169 body mass was measured every two weeks under anaesthesia (140 mg L⁻¹ benzocaine). To
170 estimate total tank biomass each day, body mass gain (or loss) was assumed to be linear
171 between successive bi-weekly measures. Total biomass was then used to adjust rations and
172 to calculate oxygen consumption. No mortality was observed during the experiments.

173 **2.3. Protocols**

174 ***2.3.1. Experiment 1: Effects of prey size, prey abundance and temperature on daily*** 175 ***energy expenditure.***

176 To investigate effects of prey size, we offered sardines one of two commercial pellets that
177 had similar composition in terms of lipids and proteins but differed in size, being either 0.2

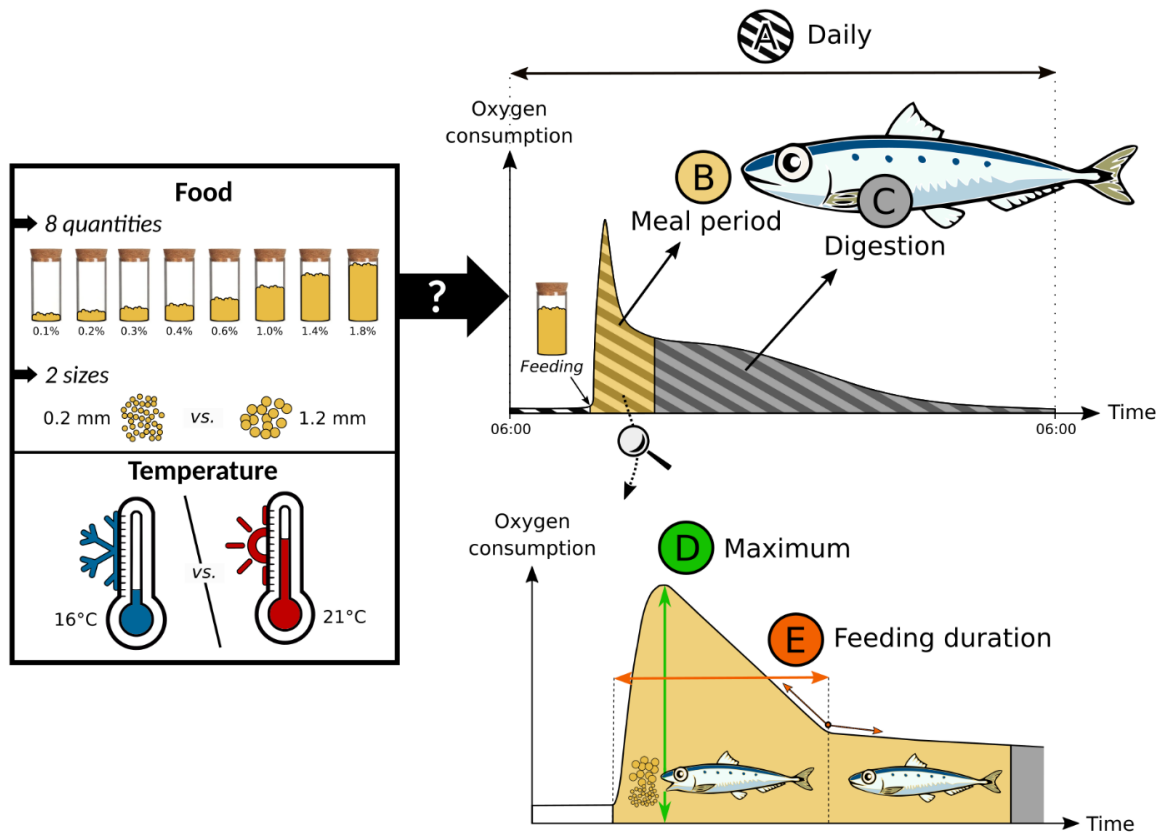
178 mm or 1.2 mm in diameter, for a period of six weeks. These sizes fall within the natural range
179 of sardine prey (Nikolioudakis et al., 2012), but elicit two markedly different foraging modes,
180 being either filtering on 0.2 mm pellets or particulate capture of 1.2 mm pellets (Queiros et
181 al., 2019). Eight prey abundances were studied, as pellet rations ranging from 0.1 to 1.8 % of
182 the total fish mass per tank: 0.1%, 0.2%, 0.3%, 0.4%, 0.6%, 1.0%, 1.4%, 1.8%. The combination
183 of two sizes and eight rations resulted in 16 feeding treatments for each of the 2 temperatures
184 (Figure 1). Sardines were fed once a day at 09:00 in the morning. Daily feeding treatment for
185 a tank was randomly assigned but comprised 2 replicates of each feeding treatment per tank
186 over the entire experiment (i.e. 8 replicates per feeding treatment x temperature).

187 The cyclical measures of oxygen uptake rate (MO_2 in $mg\ kg^{-1}\ h^{-1}$) provided an indirect estimate
188 of metabolic rate and, therefore, energy use, while the sardines fed, digested and exhibited
189 diurnal patterns of spontaneous activity. Methodological details are provided below. A
190 continual cycle of 15 min stopped flow to measure MO_2 alternated with 15 min flush with
191 aerated water was used, except at feeding when flow was stopped for 30 min (at rations of
192 0.1%, 0.2%, 0.3% and 0.4%) or 60 min (at rations of 0.6%, 1.0%, 1.4% and 1.8%), to ensure the
193 entire ration was consumed before flushing. Food was distributed 5 minutes after flow was
194 stopped, when water level had stabilized in all respirometers.

195 Bias due to behavioural responses to the act of feeding (e.g. anticipation caused by human
196 presence near tanks at the typical feeding time) was controlled for by sham-feeding events,
197 where the typical feeding gestures were performed but no food was provided. These shams
198 were performed twice a day (9:00 am and 2:00 pm) for 2 days in all tanks, in the middle and
199 at the end of experiment 1.

200 **2.3.2. Experiment 2: Effects of prey size, prey abundance and temperature on**
201 **features of foraging behaviour.**

202 In this experiment we studied features of the foraging modes, filtration or particulate capture,
203 in more detail, considering duration and maximum intensity (Figure 1). To this end, sardines
204 were fed twice a day (9:00 am and 2:00 pm) for 3 weeks with 8 treatments: one of two food
205 sizes (0.2 and 1.2 mm) at four rations (0.1, 0.2, 0.3 and 0.4% of tank biomass). The
206 combination of two sizes and four rations resulted in 8 feeding treatments for each of the 2
207 temperatures (16°C and 21°C). Based on the results of Experiment 1, rations were chosen not
208 to cause satiety. Similar to Experiment 1, MO₂ was measured throughout and for 30 min
209 during feeding (food distributed after 5 min). Combining these data with those of Experiment
210 1 (Fig. S3), we obtained a total of 24 replicates per feeding treatment x temperature for food
211 rations between 0.1% and 0.4%. Any bias due to behavioural responses to the act of feeding
212 were assessed by two sham events, as described above.



213

214 *Figure 1: Conceptual framework of the two experiments on cocktail effects of food size (0.2*
 215 *and 1.2 mm), food ratios (between 0.1% and 1.8% of the total biomass in tank) and*
 216 *temperature (16°C and 21°C) on energy expenditure of sardines (daily [A], during the meal*
 217 *period [B], during digestion [C], on the maximal intensity during feeding [D]) and on the*
 218 *duration of the feeding activity [E].*

219 **2.4. Respirometry**

220 Water oxygen levels were recorded every 5 seconds in the tank respirometers, with an O₂
 221 optode (Oxy-10 mini; PreSens Precision Sensing GmbH, /www.presens.de) and associated
 222 software (Pre-Sens Oxy 4v2). Water O₂ saturation never fell below 70% during the 15 min of
 223 stopped flow and never below 60% after feeding. Saturation was rapidly restored when the
 224 tanks were flushed with a flow of aerated water from the reservoir.

225 Oxygen uptake by the sardines caused a linear decline in water O₂ concentration over time
226 during each stopped flow phase ('closed phase'). The MO₂ was calculated in mg O₂ kg⁻¹ h⁻¹,
227 using least-square regression of the slope, considering oxygen solubility at the appropriate
228 temperature (measured continuously) and salinity (measured daily); tank volume (50 L), and
229 fish biomass (McKenzie et al., 2007). Only slopes with R² ≥ 0.95 were kept for further analyses
230 (<5% of slopes were removed from analyses). Gas exchange across the water surface being
231 negligible, no correction was applied when estimating sardine oxygen consumption
232 (McKenzie et al., 2007; Queiros et al., 2021).

233 **2.5. Respirometry data analyses**

234 ***2.5.1. Basal and daily oxygen consumption***

235 Basal O₂ uptake rate of day_i was expressed as the lowest 15%-quantile (Chabot et al., 2016a)
236 of the daily O₂ consumption of the previous day (from 06:00 a.m. day_{i-1} to 06:00 a.m. day_i).
237 This rate of oxygen uptake was then used as a baseline for calculating daily oxygen
238 consumption on day_i, expressed in mg O₂ kg⁻¹ d⁻¹, as an increase from this basal rate. This
239 normalisation avoided bias linked to a change in fish biomass during experiments, short-term
240 effects of a previous meal, or a small change in temperature, salinity, minor human
241 disturbance, etc. Daily MO₂ was calculated as the area under the curve (AUC) of MO₂ over
242 time, from 06:00 a.m. and for 24 hours (Figure 1, point A) using the '*DescTools*' package in R
243 (Andri Signorell 2021). The AUC was calculated over two periods: (i) raw data from 06:00 a.m.
244 until noon, to catch the peak of oxygen consumption observed during the meal period and (ii)
245 smoothed values of the oxygen consumption after 12:00 a.m. (oxygen consumption
246 smoothed using *lowess* function) to avoid outliers due to, for example, minor disturbance in
247 the room, that might distort daily estimations (Fig. S3).

248 **2.5.2. Oxygen consumption during feeding**

249 When focusing on effects of a meal on MO₂, these were calculated relative to a control
250 baseline that was estimated as the mean of the preceding 2.5 hours. This was done to avoid
251 bias when either lights were turned on 1.5 hour before the 1st daily meal, or there were
252 remnant effects of digestion of that 1st meal for the 2nd meal period. Since it took up to 2
253 minutes to feed all tanks (i.e. between 5 and 7 minutes after the beginning of the closed
254 phase), we first needed to establish the start of the feeding event for each tank. To do so, we
255 identified a break in the rate of oxygen decline in the water during the initial minutes of the
256 'closed phase', using the 'segmented' package (Muggeo, 2008). Once this was identified,
257 oxygen consumption was calculated, in mg O₂ kg⁻¹ h⁻¹, as the linear decline of oxygen
258 concentration from there until 2 min before the end of the 'closed phase' (Figure 1, point B).

259 **2.5.3. Oxygen consumption during digestion**

260 The start of the digestion period was considered to begin 90 min after the start of the meal
261 period, this being the maximal duration of the feeding and then flush periods across the
262 different rations. Thus, with feeding at 09:00, the oxygen consumption during digestion was
263 calculated, in mg O₂ kg⁻¹ d⁻¹, as the AUC of the oxygen consumption over time between 10:30
264 a.m. of day_i and 06:00 a.m. of day_{i+1} (Figure 1, point C). This oxygen consumption was
265 expressed as an increase from the basal O₂ uptake of day_i as estimated above.

266 **2.5.4. Maximal oxygen consumption during feeding**

267 To reveal dynamics of metabolic rate after feeding (Fig. S5), MO₂ was estimated as a moving
268 average at 30 second intervals during the closed feeding period, using linear regressions over
269 1 minute on smoothed data for 12 measures of tank oxygen concentration. This revealed the

270 maximum oxygen consumption, in $\text{mg O}_2 \text{ kg}^{-1} \text{ h}^{-1}$, achieved during each meal period (Figure 1,
271 point D).

272 ***2.5.5. Duration of the feeding period***

273 To estimate feeding duration, in minutes, we identified the end of the meal as the breakpoint
274 when oxygen concentration stopped decreasing severely after feeding, taken to indicate the
275 end of feeding-related activity (Figure 1, point E). That is, a broken-line regression was
276 performed on oxygen consumption values calculated every 30 seconds (also every 30 seconds
277 over 1 minute), starting at the peak of oxygen consumption as estimated above.

278 **2.6. Statistical analyses**

279 Effects of food rations, prey (particle) size and temperature, on oxygen consumption and
280 feeding duration, were assessed using linear mixed-effects models. We built a series of
281 models including three fixed effects (food size, food ration and temperature), as well as their
282 interactions. Because of variability among tanks within each food ration x food size x
283 temperature treatment, we also introduced a random tank intercept effect. The best-fitting
284 model was selected based on the lowest AIC_c values (Burnham and Anderson, 2002) following
285 Zuur et al. (2009). When the difference between these models in AIC_c (ΔAIC_c) was lower than
286 two, the most parsimonious model was selected (Burnham and Anderson, 2002). Food ration
287 was log-transformed for models of MO_2 during feeding and maximal MO_2 during feeding.
288 Then, food ration was second order polynomial transformed to model feeding activity.

289 Finally, the effects of prey (particle) size and temperature on oxygen consumption were
290 investigated according to 5 scenarios: (1) a change from large to small particles at cool
291 temperature; (2) a change from large to small particles at warm temperature; (3) a rise in
292 temperature with fish fed on large particles; (4) a rise in temperature with fish fed on small

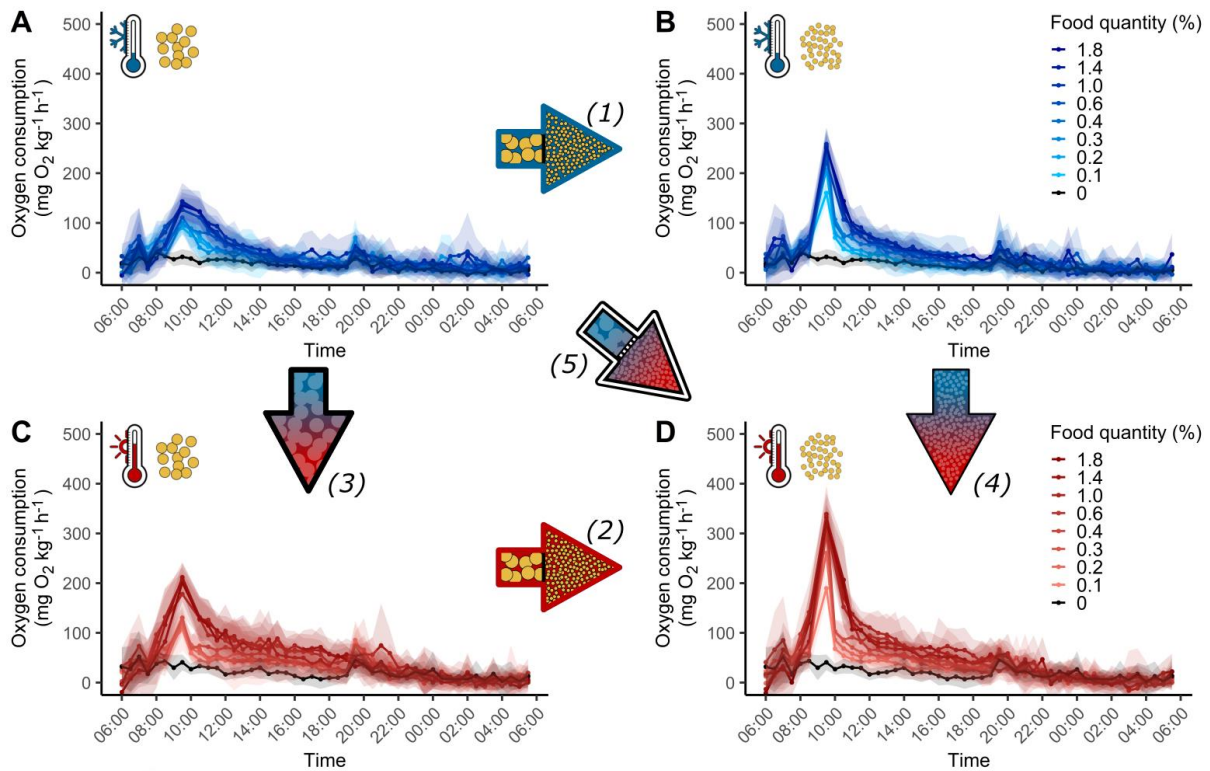
293 particles, and (5) a change from large to small particles while also increasing temperature (see
294 arrows in Figure 2). As such effects also depend on the food ration when the interaction with
295 food ration was significant, we performed pairwise comparison to test significance of
296 scenarios using selected best-fitting models as previously described. Results of scenarios over
297 food ration are expressed as absolute and relative increases. Results are indicated as mean
298 [95% CI]. Upper and lower 95% CI values of relative differences over food ration were
299 calculated following Kohavi et al. (2009).

300 All data analyses were performed under R (R Core Team, 2020) and linear mixed-effects
301 models were built using the 'lme4' package (Bates et al. 2015). All statistical tests were
302 considered significant at p-values < 0.05.

303

304 **3. Results**

305 When fasted, MO₂ was low and statistically similar throughout the day (black curve in Figure
306 2). When sardines were fed, MO₂ peaked during the feeding period after 09:00, then
307 decreased for the rest of the day for all feeding treatments and both temperatures. Oxygen
308 consumption increased with food ration and rearing temperature but, during feeding at both
309 temperatures, MO₂ was higher when feeding on the small particles (Figure 2).



310

311 *Figure 2: Median oxygen consumption over time according to food ration for the 4*
 312 *experimental treatments: cool temperature and large particles (A), cool temperature and*
 313 *small particles (B), warm temperature and large particles (C) warm temperature and small*
 314 *particles (D). Black lines are for days of fasting, blue and red represent cool (16°C) and warm*
 315 *(21°C) temperatures, respectively. Darker lines represent higher rations of food. Arrows*
 316 *represent the 5 scenarios for which oxygen consumption were compared: (1) change from*
 317 *large particles to small particles at cool temperature; (2) change from large particles to small*
 318 *particles at warm temperature; (3) rise in temperature for fish fed on large particles; (4) rise*
 319 *in temperature for fish fed on small particles, and (5) change from large particles to small*
 320 *particles while also increasing temperature.*

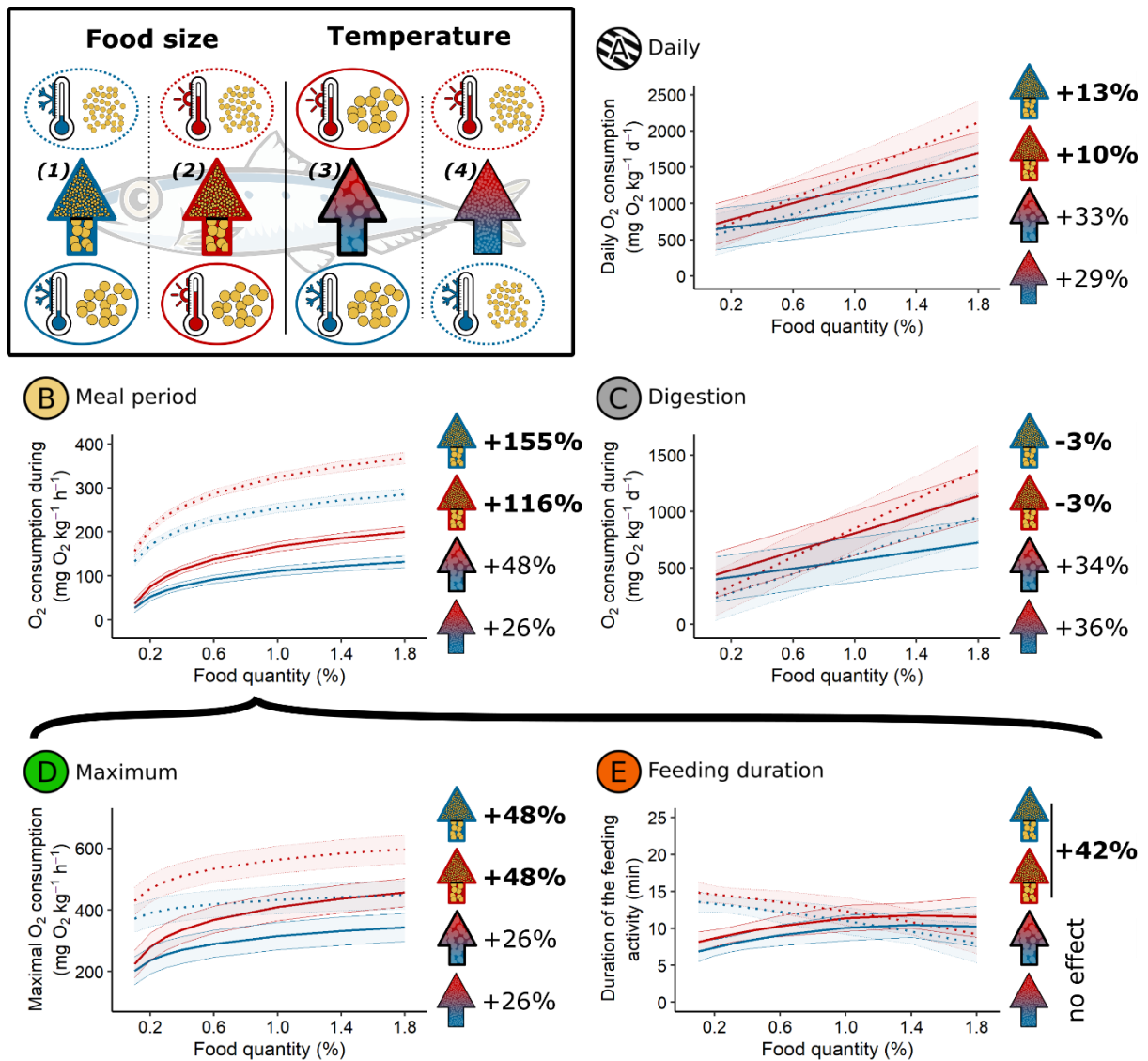
321

322 3.1. Daily oxygen consumption

323 During fasting days, median daily MO₂ (i.e. the AUC relative to basal daily oxygen
324 consumption) was the lowest, demonstrating the clear effects that feeding and/or digestion
325 exerted on daily energy expenditure (Figure 2, Fig. S6).

326 The best linear mixed-effect model included double interactions between food ration and
327 food size and between food ration and temperature (Tables S1 and S2, Fig. S6, S7). An increase
328 in ration consistently caused a significant increase in daily oxygen consumption when
329 considering either food size or temperature. When considering only food size effects, slopes
330 were significantly different ($p < 0.001$) and the increase was smaller for large particles (slope
331 [95% CI]; 420 [324;515] mg of O₂ kg⁻¹ d⁻¹) than for small particles (714 [618;810] mg of
332 O₂/kg/d, graph *Daily* in Figure 3, Table S3).

333 When comparing large to small particles over all food rations, scenarios (1) and (2) were not
334 significant since food size x temperature interaction was not retained during model selection.
335 Daily MO₂ exhibited a mean [95% CI] relative increase of 13 [1;37]% for small particles at
336 16°C, while this increase was 10 [3;22]% at 21°C (graph *Daily* in Figure 3, Table 1).



337

338 *Figure 3: Smooth functions of [A] daily, [B] while feeding, [C] while digesting, [D] maximal*

339 *oxygen consumptions (relative to basal oxygen consumption, see details in Material and*

340 *Methods) and [E] feeding duration according to the food ration for the 4 experimental*

341 *treatments: cool temperature and large particles (solid blue lines), cool temperature and small*

342 *particles (dotted blue lines), warm temperature and large particles (solid red lines) and warm*

343 *temperature and small particles (dotted red lines). Arrows represent the mean relative*

344 *increase of the oxygen consumption/feeding duration according to 4 scenarios summarized in*

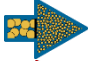



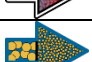




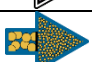
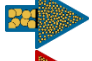



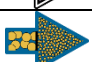
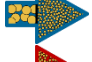



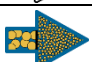


345 *top-left panel: scenario 1 = meal modification from large particles to small particles at cool*

346 *temperature, (2) meal modification from large particles to small particles at warm*

347 *temperature, (3) increasing temperature when fish fed on large particles and (4) increasing*
348 *temperature when fish fed on small particles. Only food size x food ration had a significant*
349 *effect on feeding duration.*

350

351 *Table 1: Absolute and relative differences (estimates and 95% confidence intervals) for the 5 scenarios*
 352 *for which oxygen consumption were compared: (1) change from large particles to small particles at*
 353 *cool temperature; (2) change from large particles to small particles at warm temperature; (3) rise in*
 354 *temperature for fish fed on large particles; (4) rise in temperature for fish fed on small particles, and*
 355 *(5) change from large particles to small particles while also increasing temperature. Scenarios were*
 356 *tested using pairwise comparisons. Both differences were calculated by pairwise comparisons and 95%*
 357 *CI of relative differences were estimated following Kohavi et al. 2009. Absolute differences are given*
 358 *in mg of O₂ kg⁻¹ d⁻¹ for daily and during digestion, in mg of O₂ kg⁻¹ h⁻¹ for maximal and during feeding,*
 359 *and in minutes for feeding duration.*

Period	Scenario	Relative change (%)	Absolute change
Daily	 Scenario (1): 16°C Large ⇒ Small	13 [1;37]	108 [6;211]
	 Scenario (2): 21°C Large ⇒ Small	10 [3;22]	108 [6;211]
	 Scenario (3): Large 16°C ⇒ 21°C	33 [6;87]	265 [-290;821]
	 Scenario (4): Small 16°C ⇒ 21°C	29 [8;68]	265 [-265;821]
	 Scenario (5): 16°C + Large ⇒ 21°C + Small	46 [10;121]	373 [-179;926]
Meal period	 Scenario (1): 16°C Large ⇒ Small	155 [46;397]	132 [120;143]
	 Scenario (2): 21°C Large ⇒ Small	116 [59;209]	146 [135;157]
	 Scenario (3): Large 16°C ⇒ 21°C	48 [11;128]	41 [24;58]
	 Scenario (4): Small 16°C ⇒ 21°C	26 [16;37]	56 [38;73]
	 Scenario (5): 16°C + Large ⇒ 21°C + Small	220 [68;561]	187 [170;205]
Digestion	 Scenario (1): 16°C Large ⇒ Small	-3 [-13;-1]	-18 [-112;76]
	 Scenario (2): 21°C Large ⇒ Small	-3 [-6;-1]	-18 [-112;76]
	 Scenario (3): Large 16°C ⇒ 21°C	34 [-4;183]	178 [-212;569]
	 Scenario (4): Small 16°C ⇒ 21°C	36 [-5;214]	178 [-212;569]
	 Scenario (5): 16°C + Large ⇒ 21°C + Small	31 [-3;164]	160 [-228;548]
Maximal	 Scenario (1): 16°C Large ⇒ Small	48 [24;84]	134 [111;157]
	 Scenario (2): 21°C Large ⇒ Small	48 [29;75]	170 [148;193]
	 Scenario (3): Large 16°C ⇒ 21°C	26 [12;46]	72 [-15;159]
	 Scenario (4): Small 16°C ⇒ 21°C	26 [16;39]	108 [21;195]
	 Scenario (5): 16°C + Large ⇒ 21°C + Small	87 [47;148]	242 [155;329]
Duration	  Large ⇒ Small	42 [-11;339]	4 [2;6]

360

361 **3.2. Oxygen consumption during feeding**

362 During fasting days, median MO₂ at the time of sham feeding was centered on zero (Fig. S8),
363 indicating that the increase in MO₂ observed during all true feeding events resulted from
364 actual energy expenditure to feed and not from behavioural responses by the sardines to
365 feeding gestures.

366 The MO₂ during feeding was significantly related to the three double interactions (food ration
367 x food size, food ration x temperature and food size x temperature, Tables S4 and S5, Fig. S8,
368 S9). When considering only food size effects, slopes were significantly different ($p < 0.001$)
369 and the increase was smaller for large particles (slope [95% CI]; 95 [85;105] mg of O₂ kg⁻¹ h⁻¹)
370 than for small particles (129 [119;139] mg of O₂ kg⁻¹ h⁻¹, Table S3).

371 Food size had a strong and significant effect on MO₂ during feeding. When sardines fed on
372 small particles at 16°C, their mean [95% CI] MO₂ was almost multiplied by 2.5 by comparison
373 to large particles (p -value < 0.001), rising by 155 [46;397]%, while it doubled in sardines
374 feeding on small particles, rising by 116 [59;209]% compared to large particles at 21°C (p -
375 value < 0.001 , graph *Meal period* in Figures 3, Table 1).

376 **3.3. Oxygen consumption during digestion**

377 Similar to the daily MO₂, best linear mixed-effect model for MO₂ during digestion included
378 double interactions between food ration and food size and between food ration and
379 temperature (Tables S6 and S7, Fig. S10, S11). Slopes differed significantly ($p < 0.001$); the
380 lowest slope was estimated for sardines on large particles (slope [95% CI]; 300 [213;388] mg
381 of O₂ kg⁻¹ d⁻¹) while the highest slope was obtained for sardines on small particles (533
382 [445;621] mg of O₂ kg⁻¹ d⁻¹, graph *Digestion* in Figure 3).

383 When comparing large to small particles averaged over all food rations, scenarios (1) and (2)
384 were not significant since interaction between food size and temperature was not retained in
385 the selected model. Indeed, mean [95% CI] MO₂ during digestion decreased by 3 [-13,-1]% at
386 16°C, while this decrease was 3 [-6;-1]% at 21°C (graph *Digestion* in Figure 3, Table 1).

387 **3.4. Maximal consumption during feeding**

388 Similar to the MO₂ during feeding, maximal MO₂ during feeding was significantly correlated
389 with the three double interactions (Tables S8 and S9, Fig. S12, S13). Slopes differed
390 significantly ($p = 0.001$); the lowest slope was estimated for sardines on small particles (slope
391 [95% CI]; 87 [67;106] mg of O₂ kg⁻¹ h⁻¹) while the highest slope was obtained for sardines on
392 large particles (132 [113;152] mg of O₂ kg⁻¹ h⁻¹, graph *Maximum* in Figure 3, Table S3).

393 Food size had a strong and significant effect on maximal MO₂ during feeding since food size
394 x temperature interaction was retained during model processing. When sardines fed on small
395 particles at 16°C, their mean [95% CI] maximal MO₂ rose by 48 [24;84]% by comparison to
396 large particles, while such increase was 48 [29;75]% at 21°C (graph *Maximum* in Figure 3,
397 Table 1).

398 **3.5. Feeding duration**

399 Contrary to the previous MO₂ features, the selected model for the feeding duration included
400 interaction between food ration and food size but not with temperature since food ration x
401 temperature and food size x temperature interaction were not retained (Tables S10 and S11,
402 Fig. S14, S15). Slopes differed significantly between the two food sizes ($p = 0.004$). Indeed, the
403 feeding duration decreased with increasing food ration when sardines fed on small particles
404 (slope [95% CI]; -3 [-6;0] min) while it increased when sardines fed on large particles (4 [1;7]
405 min, Table S3).

406 When comparing large to small particles averaged over all food rations, scenarios (1) and (2)
407 were not significant since interaction between food size and temperature was not retained in
408 the selected model. Mean [95% CI] feeding duration increased by 42 [-11;339]% (graph
409 *Feeding duration* in Figure 3, Table 1).

410 **3.6. Temperature effects**

411 Temperature had significant effects on all oxygen consumptions and on the feeding duration
412 (Tables S1 to S11). Indeed, food ration x temperature interaction was included in all selected
413 models on MO₂ and food size x temperature interaction was included in models on MO₂
414 during feeding and maximal MO₂ during feeding. Moreover, in the model on feeding
415 duration, temperature was retained without its interactions (Tables S10).

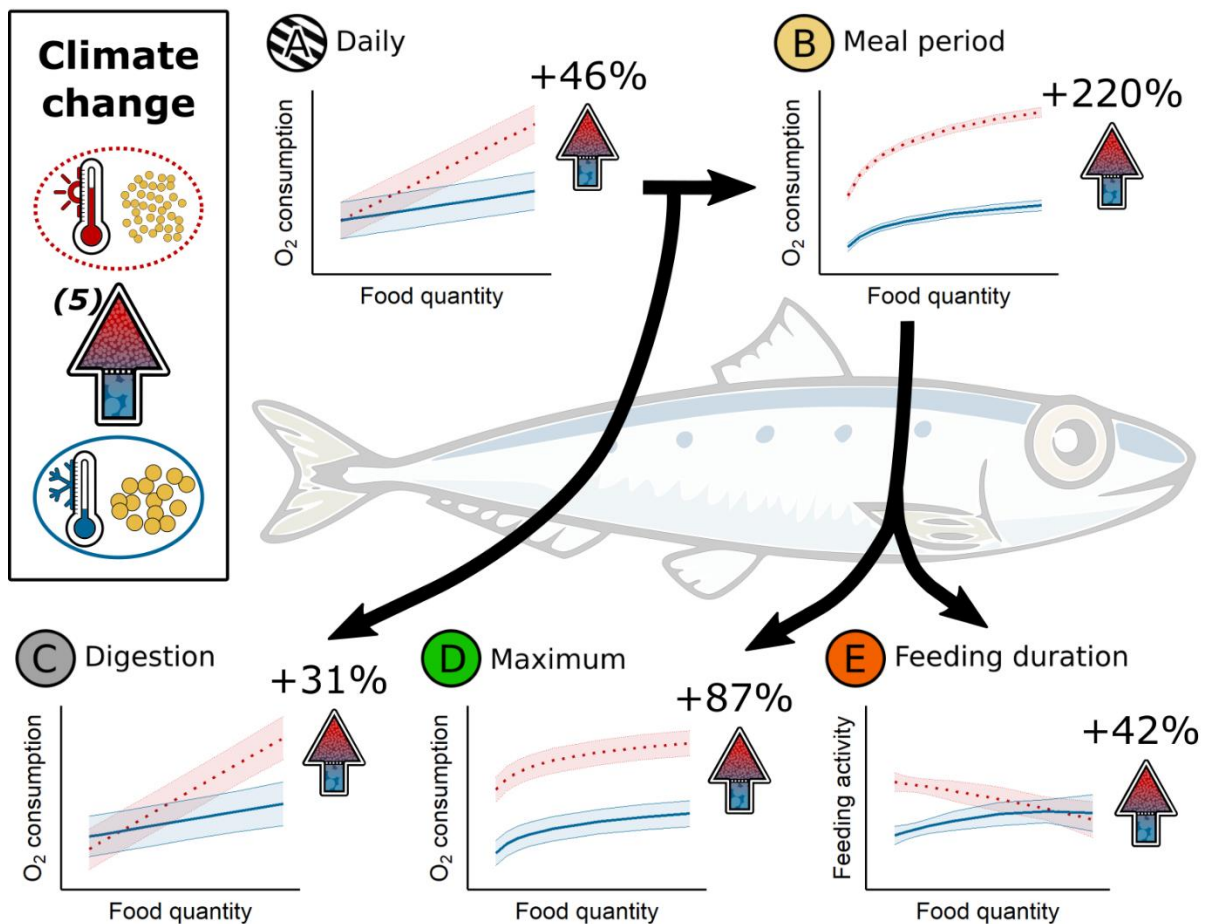
416 When studying interaction of food ration and temperature, slopes were significant different
417 between the two temperatures in all MO₂ models and they were always smaller at cool than
418 at warm temperature. Thus, slopes were smaller at 16°C than at 21°C for daily MO₂, MO₂
419 during digestion, MO₂ during feeding, and maximal MO₂ during feeding (Table S3).
420 Surprisingly, slopes were very similar when considering either large particles or cool
421 temperature effects (e.g. slopes [95% CI] for daily MO₂, 420 [324;515] and 413 [317;509],
422 respectively) and either small particles or warm temperature effects (for daily MO₂, 714
423 [618;810] and 721 [626;817], respectively, suggesting similar effects of prey shrinking and
424 temperature warming over food ration on MO₂ (see Table S3).

425 When comparing cool to warm conditions, in scenarios (3) and (4) there was no significant
426 effect of temperature on daily MO₂, MO₂ during digestion or on feeding duration, because
427 food size x temperature interaction was not retained within selected models. On the other
428 hand, warming effects were significant on MO₂ during feeding (p-values < 0.001) but only

429 scenario (4) was significant on maximal MO₂ during feeding (p-value = 0.02). Thus, the
430 temperature change from 16°C to 21°C caused mean MO₂ during feeding to increase by 26
431 [16;37]% in fish fed on small particles, and by 49 [11;129]% in fish fed on large particles. This
432 temperature change caused mean maximal MO₂ during feeding to increase by 26 [16;39]%
433 in sardines fed with small particles (Figure 3, Table 1).

434 **3.7. Cocktail effects of the global warming**

435 Smaller particle size and higher temperature resulted in a mean [95% CI] daily MO₂ increase
436 of 46 [10;121]%, representing an increase of 373 [-179;926] mg of O₂ kg⁻¹ d⁻¹. This increase
437 was caused by the significant multiplication by 3 of the MO₂ during the meal period (220
438 [68;561]%, representing 187 [170;205] mg of O₂ kg⁻¹ h⁻¹) and higher MO₂ during the digestion
439 (31 [-3;163]%, representing 160 [-228;548] mg of O₂ kg⁻¹ d⁻¹). Moreover, such change caused
440 an increase of the maximal MO₂ during feeding by 87 [47;148]%, representing an increase of
441 242 [155;329] mg of O₂ kg⁻¹ h⁻¹, and a longer feeding period (42 [-11;339]%, representing 4
442 [2;6] min without temperature effect, Figure 4, Table 1).



443

444 *Figure 4: Smooth functions of [A] daily, [B] while feeding, [C] while digesting, [D] maximal*
 445 *oxygen consumptions and [E] feeding duration according to the food ration for the 2*
 446 *experimental treatments representing past and future environmental conditions, i.e. cool*
 447 *temperature and large particles (solid blue lines) and warm temperature and small particles*
 448 *(dotted red lines), respectively. Arrows represent the mean relative increase of the oxygen*
 449 *consumption/feeding duration according to the global warming (scenario 5), i.e. meal*
 450 *modification from large particles to small particles with increasing temperature, and*
 451 *summarized in top-left panel (feeding duration is not significantly affected by temperature*
 452 *increase, see Results).*

453

454 **4. Discussion**

455 This study investigated how a modification of food resources under climate warming might
456 jeopardize energy balance of small pelagic species, using sardines in the Mediterranean Sea
457 as a case study. To do so, we used in-vivo group respirometry to investigate the effects of
458 prey (food) size and availability (ration) on sardine energy expenditure, and how this was
459 influenced by temperature. Our results demonstrate that both food size and temperature had
460 significant effects on multiple measures of energy expenditures, over daily and hourly
461 timescales. While temperature significantly increased expenditures overall, food size had a
462 major impact on energy expenditure for activity during feeding itself. That is, the results
463 indicate that food resources and temperature are major environmental drivers that can
464 dramatically increase energy expenditures of fishes and disturb their energy balance in a
465 scenario of future climate change, in warmer waters with smaller prey. As such, the results
466 also provide experimental evidence that such challenges to energy balance may contribute to
467 the ongoing shrinking of fish populations.

468 Daily oxygen consumption measured in this study was corrected against a baseline of
469 standard metabolism (Chabot et al., 2016a), so represents daily energy expenditure on
470 activity. The results suggested greater expenditure for days where sardines fed on small
471 particles, due to higher oxygen consumption during either feeding and/or digestion. The very
472 marked increase in oxygen consumption during actual feeding on small items must reflect
473 different costs of foraging mode, with filtering being more expensive than particulate feeding.
474 While this confirms our hypothesis and helps explain the decreased growth and body
475 condition of sardines fed for an extended period on small items (Queiros et al., 2019), the
476 magnitude of the effect is quite remarkable. Both MO₂ and duration of the meals provide a

477 more detailed understanding of the widely different energy costs of the two foraging modes.
478 First, the higher maximal MO₂ when fish fed on small particles indicates greater energy
479 requirements for the continuous aerobic swimming in filter-feeding compared to rapid bursts
480 to capture large particles (Costalago & Palomera, 2014). Queiros et al. (2019) had already
481 noted that the duration of feeding activity was longer when sardines fed on small particles, it
482 presumably represents the time needed to filter the entire tank volume and, therefore, might
483 not be expected to change much with ration. It is interesting therefore that feeding duration
484 on small particles was in fact lower at low or high rations than at intermediate ones. Low
485 duration at low ration might suggest rapid loss of interest if food acquisition was very poor,
486 while at high ration it might indicate satiation. For particulate feeding, more particles to catch
487 should translate into longer duration, which was observed until a ration threshold where a
488 plateau would indicate satiation. Overall, we expected feeding duration to be longer on small
489 particles at low ration but longer on large particles, but this was only true for rations below
490 0.6 %, after which duration was similar for both particle sizes. Finally, all these results indicate
491 that higher energy expenditure by sardines filter feeding on small particles can explain why
492 they would have to eat twice as much as when feeding on large pellets to achieve similar
493 growth or body condition (Queiros et al. 2019).

494 Our finding that oxygen consumption during the digestion increased with the food ration, for
495 both particle sizes, presumably reflects the so-called specific dynamic action of feeding (SDA)
496 response (McCue, 2006). This reflects the energy needed for the digestion, absorption and
497 assimilation of a meal (Chabot et al., 2016b), hence the energetic 'costs of growth'. Therefore,
498 larger meals require greater energy investment but then provide a great return in terms of
499 tissue accretion and growth (Fu et al., 2005a, 2005b; Jordan & Steffensen, 2007; Norin & Clark,

2017). The fact that a doubling of ration from 0.4% to 0.8% only caused a 17% or 55% increase in apparent SDA (based on estimated slopes), in fish fed large items at 16 °C or small items at 21°C, respectively, might seem limited. This increase with doubling of ration is low compared to other fish species (see Secor, 2009). Furthermore, the high surface area to volume ratio of small particles should speed up digestion by promoting enzymatic processes and, thereby, reduce a part of digestion costs (discussed in Legler et al., 2010). On the other hand, a large SDA response can indicate that lots of nutrients were assimilated, notably amino acids for protein synthesis, with high costs of turning these into tissues but that reflect robust growth (Fraser & Rogers, 2007; McCue, 2006; Secor, 2009). That is, a large SDA would imply good growth, which is coherent with the fact that sardines fed on large particles exhibited higher growth and greater condition in previous studies (see Queiros et al. 2019).

There is another mechanism that might increase energy expenditure during 'digestion' of large particles, being the costs of recovery from rapid bursts of anaerobic swimming used for prey capture. The metabolic cost of such recovery, so-called 'excess post-exercise oxygen consumption' (EPOC) can be divided into 3 phases in fishes: rapid, plateau, slow (Zhang et al., 2018). While the rapid phase is very short (< 1 hour), both plateau and slow phases can require several hours to return to standard metabolism. This can be more than 10 hours for salmon although the duration is certainly species dependent (C. G. Lee et al., 2003; Li et al., 2020; Plambech et al., 2013; Svendsen et al., 2012; Zhang et al., 2018). Considering that we estimated energy expenditure of digestion starting at 1.5 hours after providing the meal, this would omit the rapid phase of EPOC, although the phenomenon may have contributed to the final phases of metabolic costs of feeding. A potential role for EPOC in costs of feeding on large prey remains to be proven, since studies on individual sardines are technically extremely

523 challenging. Overall, oxygen consumption due to digestion was lower for small compared to
524 large particles, but the magnitude of the difference was much less than for the activity costs
525 of feeding. Therefore, daily energy expenditure was mostly affected by what happened during
526 the meal. The benefit of digesting small prey (in terms of energy expenditure for a same food
527 ration) remained too weak to counterbalance the increased energy to capture shrinking
528 plankton in the wild. Furthermore, the warm temperature also significantly increased
529 metabolic rates, leading to overall higher energy expenditure during both meals and digestion
530 (Clarke & Fraser, 2004; Seebacher et al., 2015), whatever the food size or ration. Higher
531 energetic cost for digestion at warm temperatures has been reported for tunas, another
532 species that swims continuously (Klinger et al., 2016) although relationships between costs of
533 digestion and temperature are not necessarily linear (McKenzie et al., 2013; Tirsgaard et al.,
534 2015).

535 Our study applied relatively short thermal acclimation times, which might tend to
536 overestimate temperature effects. When natural populations are allowed to acclimatise over
537 generations, baseline metabolism may show a much less marked effect of temperature (e.g.
538 Wootton et al. 2022). Such intergenerational experiments are not feasible for the
539 Mediterranean sardine because their life cycle cannot be completed in captivity. Our
540 experimental temperatures (16°C and 21°C) were well within the range that sardines have
541 experienced in the Gulf of Lions over the last 40 years (12 - 24°C ; Feuilleley et al. 2020) and
542 our rate of temperature change was slow (< 0.5°C/day) allowing acclimation at an ecologically
543 realistic pace. Furthermore, by expressing oxygen consumption as a relative increase from
544 MO₂ baseline (the baseline was estimated daily as the lowest 15%-quantile rate for daily MO₂
545 and MO₂ during digestion, and as the mean of the preceding 2.5 hours for MO₂ while

546 feeding), effects of temperature on baseline metabolism were been taken into account in our
547 study. Finally, although the effects of temperature were significant, potential acclimation
548 across a few generations leading to similar baseline metabolism between generations would
549 reinforce our results on the effects of food size.

550 Although food size had only quite minor effects on daily energy use, increasing it by 10 [3;22]%
551 in fish fed on small particles at 21°C, long-term effects may be significant. Furthermore,
552 sardines may feed continuously in the wild, not only once or twice a day, which would
553 increase consequences of differences in energy expenditure during feeding. In the wild,
554 sardines face predation and pathogens that require energy expenditure. Therefore, higher
555 daily energy expenditure for feeding may well impair energy balance in the wild, resulting in
556 less energy allocated towards survival and growth. For instance, lower swimming
557 performance due to low energy reserves (e.g. swimming endurance (Martínez et al., 2003,
558 2004)) could isolate leaner individuals from schools, leading to a vicious circle, with lower
559 food foraging and thus reinforcing lower energy reserves. Nonetheless, calorie-restricted
560 sardines display better phenotypic plasticity to face fasting, which improves their ability to
561 reduce their metabolic energy expenditures during long-term fasting (Queiros et al., 2021).
562 Further, mitochondria from sardines fed with small particles exhibited lower basal oxidative
563 activity but higher efficiency of ATP production than those fed with large particles, a
564 mechanism that should help them spare energy (Thoral et al., 2021). Nevertheless, although
565 sardines may display plasticity or adaptation that ameliorates the energetic consequences of
566 smaller prey and warmer temperatures, the situation of sardine populations in the Gulf of
567 Lions remains very concerning.

568

569 **Conclusion**

570 This study supports the hypothesis of bottom-up control to explain the profound shrinking of
571 small pelagic fish communities in the Gulf of Lions and is a hypothesis worth exploring to
572 explain the spread of this phenomenon throughout the Mediterranean (Albo-Puigserver et
573 al., 2021; Brosset et al., 2017) to new ecosystems, and to species higher in the food web
574 (Bensebaini et al., 2022; Véron et al., 2020). Altogether, the results indicate that energy
575 balance can be a major mechanism explaining shrinking of fish populations globally. Declines
576 in prey size could impact the energy balance of individuals when their energy expenditures
577 are increased by warmer temperatures, with future projections of prey resources predicting
578 a decline of prey biomass and quality.

579 **Acknowledgments**

580 We would like to thank colleagues at the IFREMER experimental station for their welcome
581 and their fruitful advice during the conceptualization of the experiments. We would also like
582 to express our thanks to the two anonymous reviewers for their comments that helped us
583 improve the manuscript.

584 **Funding**

585 The study was funded by the MUSE Key Initiative Sea and Coast.

586

587 **Data availability**

588 Data and scripts are available here: <https://zenodo.org/record/8413664>.

589 5. References

- 590 Albo-Puigserver, M., Pennino, M. G., Bellido, J. M., Colmenero, A. I., Giráldez, A., Hidalgo,
591 M., Gabriel Ramírez, J., Steenbeek, J., Torres, P., Cousido-Rocha, M., & Coll, M. (2021).
592 Changes in Life History Traits of Small Pelagic Fish in the Western Mediterranean Sea.
593 *Frontiers in Marine Science*, 8, 1197.
594 <https://doi.org/10.3389/FMARS.2021.570354/BIBTEX>
- 595 Alheit, J., Roy, C., & Kifani, S. (2009). Decadal-scale variability in populations. In D.
596 Checkley, J. Alheit, Y. Oozeki, & C. Roy (Eds.), *Climate Change and Small Pelagic Fish* (pp.
597 64–87). Cambridge University Press.
- 598 Allison, E. H., Perry, A. L., Badjeck, M. C., Neil Adger, W., Brown, K., Conway, D., Halls, A.
599 S., Pilling, G. M., Reynolds, J. D., Andrew, N. L., & Dulvy, N. K. (2009). Vulnerability of
600 national economies to the impacts of climate change on fisheries. *Fish and Fisheries*,
601 10(2), 173–196. <https://doi.org/10.1111/j.1467-2979.2008.00310.x>
- 602 Andri Signorell (2023). DescTools: Tools for Descriptive Statistics (R package version
603 0.99.49). <https://cran.r-project.org/package=DescTools>
- 604 Ariza, A., Lengaigne, M., Menkes, C., Lebourges-Dhaussy, A., Receveur, A., Gorgues, T.,
605 Habasque, J., Gutiérrez, M., Maury, O., & Bertrand, A. (2022). Global decline of pelagic
606 fauna in a warmer ocean. *Nature Climate Change*. [https://doi.org/10.1038/S41558-022-](https://doi.org/10.1038/S41558-022-01479-2)
607 01479-2
- 608 Atkinson, D. (1994). Temperature and Organism Size—A Biological Law for Ectotherms?
609 In *Advances in Ecological Research* (Vol. 25, Issue C, pp. 1–58).
610 [https://doi.org/10.1016/S0065-2504\(08\)60212-3](https://doi.org/10.1016/S0065-2504(08)60212-3)
- 611 Audzijonyte, A., Richards, S. A., Stuart-Smith, R. D., Pecl, G., Edgar, G. J., Barrett, N. S.,
612 Payne, N., & Blanchard, J. L. (2020). Fish body sizes change with temperature but not all
613 species shrink with warming. *Nature Ecology and Evolution*, 4(6), 809–814.
614 <https://doi.org/10.1038/s41559-020-1171-0>
- 615 Bates, D., Mächler, M., Bolker, B., Walker, S., 2015. Fitting Linear Mixed-Effects Models
616 Using lme4. *J Stat Softw*. <https://doi.org/10.18637/jss.v067.i01>
- 617 Baudron, A. R., Needle, C. L., Rijnsdorp, A. D., & Tara Marshall, C. (2014). Warming
618 temperatures and smaller body sizes: synchronous changes in growth of {North} {Sea}
619 fishes. *Global Change Biology*, 20(4), 1023–1031. <https://doi.org/10.1111/gcb.12514>
- 620 Bensebaini, C. M., Certain, G., Billet, N., Jadaud, A., Gourguet, S., Hattab, T., & Fromentin,
621 J. M. (2022). Interactions between demersal fish body condition and density during the
622 regime shift of the Gulf of Lions. *ICES Journal of Marine Science*.
623 <https://doi.org/10.1093/icesjms/fsac106>

- 624 Bopp, L., Aumont, O., Cadule, P., Alvain, S., & Gehlen, M. (2005). Response of diatoms
625 distribution to global warming and potential implications: A global model study.
626 *Geophysical Research Letters*, 32(19), n/a-n/a. <https://doi.org/10.1029/2005GL023653>
- 627 Bopp, L., Resplandy, L., Orr, J. C., Doney, S. C., Dunne, J. P., Gehlen, M., Halloran, P.,
628 Heinze, C., Ilyina, T., Séférian, R., Tjiputra, J., & Vichi, M. (2013). Multiple stressors of
629 ocean ecosystems in the 21st century: projections with CMIP5 models. *Biogeosciences*,
630 10(10), 6225–6245. <https://doi.org/10.5194/bg-10-6225-2013>
- 631 Brochier, T., Echevin, V., Tam, J., Chaigneau, A., Goubanova, K., & Bertrand, A. (2013).
632 Climate change scenarios experiments predict a future reduction in small pelagic fish
633 recruitment in the Humboldt Current system. *Global Change Biology*, 19(6), 1841–1853.
634 <https://doi.org/10.1111/gcb.12184>
- 635 Brosset, P., Fromentin, J.-M., van Beveren, E., Lloret, J., Marques, V., Basilone, G.,
636 Bonanno, A., Carpi, P., Donato, F., Čikeš Keč, V., de Felice, A., Ferreri, R., Gašparević, D.,
637 Giráldez, A., Gücü, A., Iglesias, M., Leonori, I., Palomera, I., Somarakis, S., ... Saraux, C.
638 (2017). Spatio-temporal patterns and environmental controls of small pelagic fish body
639 condition from contrasted Mediterranean areas. *Progress in Oceanography*, 151, 149–
640 162. <https://doi.org/10.1016/j.pocean.2016.12.002>
- 641 Brosset, P., le Bourg, B., Costalago, D., Bănaru, D., van Beveren, E., Bourdeix, J.,
642 Fromentin, J., Ménard, F., & Saraux, C. (2016). Linking small pelagic dietary shifts with
643 ecosystem changes in the Gulf of Lions. *Marine Ecology Progress Series*, 554, 157–171.
644 <https://doi.org/10.3354/meps11796>
- 645 Burnham, K.P., Anderson, D.R., 2004. Model Selection and Multimodel Inference, 2nd
646 ed. ed. Springer New York, New York, NY. <https://doi.org/10.1007/b97636>
- 647 Chabot, D., Steffensen, J. F., & Farrell, A. P. (2016a). The determination of standard
648 metabolic rate in fishes. *Journal of Fish Biology*, 88(1), 81–121.
649 <https://doi.org/10.1111/jfb.12845>
- 650 Chabot, D., Koenker, R., & Farrell, A. P. (2016b). The measurement of specific dynamic
651 action in fishes. *Journal of Fish Biology*, 88(1), 152–172.
652 <https://doi.org/10.1111/JFB.12836>
- 653 Clarke, A., & Fraser, K. P. P. (2004). Why does metabolism scale with temperature?
654 *Functional Ecology*, 18(2), 243–251. <https://doi.org/10.1111/j.0269-8463.2004.00841.x>
- 655 Costalago, D., Garrido, S., & Palomera, I. (2015). Comparison of the feeding apparatus
656 and diet of European sardines *Sardina pilchardus* of Atlantic and Mediterranean waters:
657 Ecological implications. *Journal of Fish Biology*, 86(4), 1348–1362.
658 <https://doi.org/10.1111/jfb.12645>

659 Costalago, D., & Palomera, I. (2014). Feeding of European pilchard (*Sardina pilchardus*)
660 in the northwestern Mediterranean: from late larvae to adults. *Scientia Marina*, 78(1),
661 41–54. <https://doi.org/10.3989/scimar.03898.06D>

662 Daufresne, M., Lengfellner, K., & Sommer, U. (2009). Global warming benefits the small
663 in aquatic ecosystems. *Proceedings of the National Academy of Sciences*, 106(31),
664 12788–12793. <https://doi.org/10.1073/pnas.0902080106>

665 Diamond, S. E., & Kingsolver, J. G. (2010). Environmental Dependence of Thermal
666 Reaction Norms: Host Plant Quality Can Reverse the Temperature-Size Rule. *The*
667 *American Naturalist*, 175(1), 1–10. <https://doi.org/10.1086/648602>

668 FAO. (2018). The State of World Fisheries and Aquaculture 2018 - Meeting the
669 sustainable development goals. 210 pp.

670 Feuilloley, G., Fromentin, J. M., Stemmann, L., Demarcq, H., Estournel, C., & Saraux, C.
671 (2020). Concomitant changes in the environment and small pelagic fish community of
672 the Gulf of Lions. *Progress in Oceanography*, 186, 102375.
673 <https://doi.org/10.1016/j.pocean.2020.102375>

674 Forster, J., Hirst, A. G., & Atkinson, D. (2012). Warming-induced reductions in body size
675 are greater in aquatic than terrestrial species. *Proceedings of the National Academy of*
676 *Sciences*, 109(47), 19310–19314. <https://doi.org/10.1073/pnas.1210460109>

677 Fraser, K. P. P., & Rogers, A. D. (2007). Protein Metabolism in Marine Animals: The
678 Underlying Mechanism of Growth. *Advances in Marine Biology*, 52, 267–362.
679 [https://doi.org/10.1016/S0065-2881\(06\)52003-6](https://doi.org/10.1016/S0065-2881(06)52003-6)

680 Fréon, P., Cury, P. M., Shannon, L. J., & Roy, C. (2005). Sustainable exploitation of small
681 pelagic fish stocks challenged by environmental and ecosystem changes: a review.
682 *Bulletin of Marine Science*, 76(2), 385–462.

683 Fu, S. J., Xie, X. J., & Cao, Z. D. (2005a). Effect of meal size on postprandial metabolic
684 response in southern catfish (*Silurus meridionalis*). *Comparative Biochemistry and*
685 *Physiology Part A: Molecular & Integrative Physiology*, 140(4), 445–451.
686 <https://doi.org/10.1016/j.cbpb.2005.02.008>

687 Fu, S. J., Xie, X. J., & Cao, Z. D. (2005b). Effect of feeding level and feeding frequency on
688 specific dynamic action in *Silurus meridionalis*. *Journal of Fish Biology*, 67(1), 171–181.
689 <https://doi.org/10.1111/j.0022-1112.2005.00722.x>

690 Gardner, J. L., Peters, A., Kearney, M. R., Joseph, L., & Heinsohn, R. (2011). Declining body
691 size: a third universal response to warming? *Trends in Ecology & Evolution*, 26(6), 285–
692 291. <https://doi.org/10.1016/j.tree.2011.03.005>

693 Garrido, S., Ben-Hamadou, R., Oliveira, P. B., Cunha, M. E., Chícharo, M. A., & van der
694 Lingen, C. D. (2008). Diet and feeding intensity of sardine *Sardina pilchardus*: Correlation
695 with satellite-derived chlorophyll data. *Marine Ecology Progress Series*, 354, 245–256.
696 <https://doi.org/10.3354/meps07201>

697 Garrido, S., Marçalo, A., Zwolinski, J., & van der Lingen, C. (2007). Laboratory
698 investigations on the effect of prey size and concentration on the feeding behaviour of
699 *Sardina pilchardus*. *Marine Ecology Progress Series*, 330, 189–199.
700 <https://doi.org/10.3354/meps330189>

701 Horne, C. R., Hirst, Andrew. G., & Atkinson, D. (2015). Temperature-size responses match
702 latitudinal-size clines in arthropods, revealing critical differences between aquatic and
703 terrestrial species. *Ecology Letters*, 18(4), 327–335. <https://doi.org/10.1111/ele.12413>

704 IPCC. (2013). Climate Change 2013: The Physical Science Basis. Contribution of Working
705 Group I to the Fifth Assessment Report of the Intergovernmental Panel on Climate
706 Change (V. B. and P. M. M. Stocker, T.F., D. Qin, G.-K. Plattner, M. Tignor, S.K. Allen, J.
707 Boschung, A. Nauels, Y. Xia, Ed.). Cambridge University Press.

708 IPCC. (2014). Climate Change 2014: Synthesis Report. Contribution of Working Groups I,
709 II and III to the Fifth Assessment Report of the Intergovernmental Panel on Climate
710 Change . <https://www.ipcc.ch/report/ar5/syr/>

711 Jordan, A. D., & Steffensen, J. F. (2007). Effects of Ration Size and Hypoxia on Specific
712 Dynamic Action in the Cod. <https://doi.org/10.1086/510565>, 80(2), 178–185.
713 <https://doi.org/10.1086/510565>

714 Klinger, D. H., Dale, J. J., Gleiss, A. C., Brandt, T., Estess, E. E., Gardner, L., Machado, B.,
715 Norton, A., Rodriguez, L., Stiltner, J., Farwell, C., & Block, B. A. (2016). The effect of
716 temperature on postprandial metabolism of yellowfin tuna (*Thunnus albacares*).
717 *Comparative Biochemistry and Physiology Part A: Molecular & Integrative Physiology*,
718 195, 32–38. <https://doi.org/10.1016/j.cbpa.2016.01.005>

719 Kohavi, R., Longbotham, R., Sommerfield, D., Henne, R.M., 2009. Controlled experiments
720 on the web: survey and practical guide. *Data Min Knowl Discov* 18, 140–181.
721 <https://doi.org/10.1007/s10618-008-0114-1>

722 Lee, C. G., Farrell, A. P., Lotto, A., Hinch, S. G., & Healey, M. C. (2003). Excess post-exercise
723 oxygen consumption in adult sockeye (*Oncorhynchus nerka*) and coho (*O. kisutch*)
724 salmon following critical speed swimming. *Journal of Experimental Biology*, 206(18),
725 3253–3260. <https://doi.org/10.1242/JEB.00548>

726 Lee, K. P., Jang, T., Ravzanaadii, N., & Rho, M. S. (2015). Macronutrient Balance
727 Modulates the Temperature-Size Rule in an Ectotherm. *The American Naturalist*, 186(2),
728 212–222. <https://doi.org/10.1086/682072>

729 Legler, N. D., Johnson, T. B., Heath, D. D., & Ludsin, S. A. (2010). Water Temperature and
730 Prey Size Effects on the Rate of Digestion of Larval and Early Juvenile Fish. *Transactions*
731 *of the American Fisheries Society*, 139(3), 868–875. <https://doi.org/10.1577/T09-212.1>

732 Li, X., Zhang, Y., & Fu, S. (2020). Effects of short-term fasting on spontaneous activity and
733 excess post-exercise oxygen consumption in four juvenile fish species with different
734 foraging strategies. *Biology Open*, 9(9). <https://doi.org/10.1242/BIO.051755/225755>

735 Ljungström, G., Claireaux, M., Fiksen, Ø., & Jørgensen, C. (2020). Body size adaptations
736 under climate change: zooplankton community more important than temperature or
737 food abundance in model of a zooplanktivorous fish. *Marine Ecology Progress Series*,
738 636, 1–18. <https://doi.org/10.3354/meps13241>

739 Lotze, H. K., Tittensor, D. P., Bryndum-Buchholz, A., Eddy, T. D., Cheung, W. W. L.,
740 Galbraith, E. D., Barange, M., Barrier, N., Bianchi, D., Blanchard, J. L., Bopp, L., Büchner,
741 M., Bulman, C. M., Carozza, D. A., Christensen, V., Coll, M., Dunne, J. P., Fulton, E. A.,
742 Jennings, S., ... Worm, B. (2019). Global ensemble projections reveal trophic
743 amplification of ocean biomass declines with climate change. *Proceedings of the*
744 *National Academy of Sciences*, 116(26), 12907–12912.
745 <https://doi.org/10.1073/pnas.1900194116>

746 Martínez, M., Bédard, M., Dutil, J.-D., & Guderley, H. (2004). Does condition of Atlantic
747 cod (*Gadus morhua*) have a greater impact upon swimming performance at Ucrit or
748 sprint speeds? *Journal of Experimental Biology*, 207(17), 2979–2990.
749 <https://doi.org/10.1242/jeb.01142>

750 Martínez, M., Guderley, H., Dutil, J. D., Winger, P. D., He, P., & Walsh, S. J. (2003).
751 Condition, prolonged swimming performance and muscle metabolic capacities of cod
752 *Gadus morhua*. *Journal of Experimental Biology*, 206(3), 503–511.
753 <https://doi.org/10.1242/JEB.00098>

754 McCue, M. D. (2006). Specific dynamic action: A century of investigation. *Comparative*
755 *Biochemistry and Physiology Part A: Molecular & Integrative Physiology*, 144(4), 381–
756 394. <https://doi.org/10.1016/J.CBPA.2006.03.011>

757 McKenzie, D. J., Estivales, G., Svendsen, J. C., Steffensen, J. F., & Agnèse, J. F. (2013). Local
758 adaptation to altitude underlies divergent thermal physiology in tropical killifishes of the
759 genus *Aphyosemion*. *PLoS One*, 8(1). <https://doi.org/10.1371/JOURNAL.PONE.0054345>

760 McKenzie, D. J., Höglund, E., Dupont-Prinet, A., Larsen, B. K., Skov, P. V., Pedersen, P. B.,
761 & Jokumsen, A. (2012). Effects of stocking density and sustained aerobic exercise on
762 growth, energetics and welfare of rainbow trout. *Aquaculture*, 338–341, 216–222.
763 <https://doi.org/10.1016/j.aquaculture.2012.01.020>

- 764 McKenzie, D. J., Pedersen, P. B., & Jokumsen, A. (2007). Aspects of respiratory physiology
765 and energetics in rainbow trout (*Oncorhynchus mykiss*) families with different size-at-
766 age and condition factor. *Aquaculture*, 263(1–4), 280–294.
767 <https://doi.org/10.1016/j.aquaculture.2006.10.022>
- 768 Millien, V., Kathleen Lyons, S., Olson, L., Smith, F. A., Wilson, A. B., & Yom-Tov, Y. (2006).
769 Ecotypic variation in the context of global climate change: revisiting the rules. *Ecology*
770 *Letters*, 9(7), 853–869. <https://doi.org/10.1111/J.1461-0248.2006.00928.X>
- 771 Morrongiello, J. R., Sweetman, P. C., & Thresher, R. E. (2019). Fishing constrains
772 phenotypic responses of marine fish to climate variability. *Journal of Animal Ecology*,
773 88(11), 1645–1656. <https://doi.org/10.1111/1365-2656.12999>
- 774 Muggeo, V. M. R. (2008). segmented: an R Package to Fit Regression Models with Broken-
775 Line Relationships. *R News*, 8(1), 20–25. <https://cran.r-project.org/doc/Rnews/>
- 776 Nikolioudakis, N., Isari, S., Pitta, P., & Somarakis, S. (2012). Diet of sardine *Sardina*
777 *pilchardus*: An “end-to-end” field study. *Marine Ecology Progress Series*, 453, 173–188.
778 <https://doi.org/10.3354/meps09656>
- 779 Norin, T., & Clark, T. D. (2017). Fish face a trade-off between ‘eating big’ for growth
780 efficiency and ‘eating small’ to retain aerobic capacity. *Biology Letters*, 13(9).
781 <https://doi.org/10.1098/RSBL.2017.0298>
- 782 Orr, J. C., Fabry, V. J., Aumont, O., Bopp, L., Doney, S. C., Feely, R. A., Gnanadesikan, A.,
783 Gruber, N., Ishida, A., Joos, F., Key, R. M., Lindsay, K., Maier-Reimer, E., Matear, R.,
784 Monfray, P., Mouchet, A., Najjar, R. G., Plattner, G.-K., Rodgers, K. B., ... Yool, A. (2005).
785 Anthropogenic ocean acidification over the twenty-first century and its impact on
786 calcifying organisms. *Nature*, 437(7059), 681–686.
787 <https://doi.org/10.1038/nature04095>
- 788 Pauly, D., International Ecology Inst., O., Kinne, O., & Jorgensen, B. B. (2010). *Gasping*
789 *fish and panting squids: oxygen, temperature and the growth of water-breathing*
790 *animals*. <https://doi.org/10.3/JQUERY-UI.JS>
- 791 Plambech, M., van Deurs, M., Steffensen, J. F., Tirsgaard, B., & Behrens, J. W. (2013).
792 Excess post-hypoxic oxygen consumption in Atlantic cod *Gadus morhua*. *Journal of Fish*
793 *Biology*, 83(2), 396–403. <https://doi.org/10.1111/jfb.12171>
- 794 Queiros, Q., Fromentin, J.-M., Gasset, E., Dutto, G., Huiban, C., Metral, L., Leclerc, L.,
795 Schull, Q., McKenzie, D. J., & Saraux, C. (2019). Food in the Sea: Size Also Matters for
796 Pelagic Fish. *Frontiers in Marine Science*, 6. <https://doi.org/10.3389/fmars.2019.00385>
- 797 Queiros, Q., Saraux, C., Dutto, G., Gasset, E., Marguerite, A., Brosset, P., Fromentin, J.-M.
798 M., & McKenzie, D. J. (2021). Is starvation a cause of overmortality of the Mediterranean

799 sardine? *Marine Environmental Research*, 170, 105441.
800 <https://doi.org/10.1016/j.marenvres.2021.105441>

801 R Core Team. (2020). R: A Language and Environment for Statistical Computing.
802 <https://www.r-project.org/>

803 Richardson, A. J., & Schoeman, D. S. (2004). Climate Impact on Plankton Ecosystems in
804 the Northeast Atlantic. *Science*, 305(5690), 1609–1612.
805 <https://doi.org/10.1126/science.1100958>

806 Roemmich, D., & McGowan, J. (1995). Climatic Warming and the Decline of Zooplankton
807 in the California Current. *Science*, 267(5202), 1324–1326.
808 <https://doi.org/10.1126/science.267.5202.1324>

809 Saraux, C., van Beveren, E., Brosset, P., Queiros, Q., Bourdeix, J.-H., Dutto, G., Gasset, E.,
810 Jac, C., Bonhommeau, S., & Fromentin, J.-M. (2019). Small pelagic fish dynamics: A
811 review of mechanisms in the Gulf of Lions. *Deep Sea Research Part II: Topical Studies in*
812 *Oceanography*, 159, 52–61. <https://doi.org/10.1016/j.dsr2.2018.02.010>

813 Schwartzlose, R. A., Alheit, J., Bakun, A., Baumgartner, T. R., Cloete, R., Crawford, R. J.
814 M., Fletcher, W. J., Green-Ruiz, Y., Hagen, E., Kawasaki, T., Lluch-Belda, D., Lluch-Cota, S.
815 E., MacCall, A. D., Matsuura, Y., Nevárez-Martínez, M. O., Parrish, R. H., Roy, C., Serra, R.,
816 Shust, K. v., ... Zuzunaga, J. Z. (1999). Worldwide large-scale fluctuations of sardine and
817 anchovy populations. *South African Journal of Marine Science*, 21(1), 289–347.
818 <https://doi.org/10.2989/025776199784125962>

819 Secor, S. M. (2009). Specific dynamic action: A review of the postprandial metabolic
820 response. *Journal of Comparative Physiology B: Biochemical, Systemic, and*
821 *Environmental Physiology*, 179(1), 1–56. <https://doi.org/10.1007/s00360-008-0283-7>

822 Seebacher, F., White, C. R., & Franklin, C. E. (2015). Physiological plasticity increases
823 resilience of ectothermic animals to climate change. *Nature Climate Change*, 5(1), 61–
824 66. <https://doi.org/10.1038/nclimate2457>

825 Shannon, L. J., Coll, M., Neira, S., Cury, P. M., & Roux, J.-P. (2009). Impacts of fishing and
826 climate change explored using trophic models. In D. Checkley, J. Alheit, Y. Oozeki, & C.
827 Roy (Eds.), *Climate Change and Small Pelagic Fish* (pp. 158–190). Cambridge University
828 Press.

829 Sheridan, J. A., & Bickford, D. (2011). Shrinking body size as an ecological response to
830 climate change. *Nature Climate Change*, 1(8), 401–406.
831 <https://doi.org/10.1038/nclimate1259>

832 Stearns, S. C. (1989). Trade-Offs in Life-History Evolution. *Functional Ecology*, 3(3), 259.
833 <https://doi.org/10.2307/2389364>

834 Stearns, S. C. (1992). *The evolution of life histories*. Oxford University Press.
835 [http://www.sidalc.net/cgi-](http://www.sidalc.net/cgi-bin/wxis.exe/?IsisScript=sibe01.xis&method=post&formato=2&cantidad=1&expresion=mfn=007580)
836 [bin/wxis.exe/?IsisScript=sibe01.xis&method=post&formato=2&cantidad=1&expresion=](http://www.sidalc.net/cgi-bin/wxis.exe/?IsisScript=sibe01.xis&method=post&formato=2&cantidad=1&expresion=mfn=007580)
837 [mfn=007580](http://www.sidalc.net/cgi-bin/wxis.exe/?IsisScript=sibe01.xis&method=post&formato=2&cantidad=1&expresion=mfn=007580)

838 Steffensen, J. F. (1989). Some errors in respirometry of aquatic breathers: How to avoid
839 and correct for them. *Fish Physiology and Biochemistry*, 6(1), 49–59.
840 <https://doi.org/10.1007/BF02995809>

841 Svendsen, J. C., Steffensen, J. F., Aarestrup, K., Frisk, M., Etzerodt, A., & Jyde, M. (2012).
842 Excess posthypoxic oxygen consumption in rainbow trout (*Oncorhynchus mykiss*):
843 Recovery in normoxia and hypoxia. *Canadian Journal of Zoology*, 90(1), 1–11.
844 <https://doi.org/10.1139/Z11-095/ASSET/IMAGES/Z11-095TAB1.GIF>

845 Thorat, E., Queiros, Q., Roussel, D., Dutto, G., Gasset, E., McKenzie, D. J., Romestaing, C.,
846 Fromentin, J., Saraux, C., & Teulier, L. (2021). Changes in foraging mode caused by a
847 decline in prey size have major bioenergetic consequences for a small pelagic fish.
848 *Journal of Animal Ecology*, 1365-2656.13535. <https://doi.org/10.1111/1365-2656.13535>

849 Tirsgaard, B., Svendsen, J. C., & Steffensen, J. F. (2015). Effects of temperature on specific
850 dynamic action in Atlantic cod *Gadus morhua*. *Fish Physiology and Biochemistry*, 41(1),
851 41–50. <https://doi.org/10.1007/s10695-014-0004-y>

852 van Beveren, E., Bonhommeau, S., Fromentin, J.-M., Bigot, J.-L., Bourdeix, J.-H., Brosset,
853 P., Roos, D., & Saraux, C. (2014). Rapid changes in growth, condition, size and age of small
854 pelagic fish in the Mediterranean. *Marine Biology*, 161(8), 1809–1822.
855 <https://doi.org/10.1007/s00227-014-2463-1>

856 Verberk, W. C. E. P., Atkinson, D., Hoefnagel, K. N., Hirst, A. G., Horne, C. R., & Siepel, H.
857 (2021). Shrinking body sizes in response to warming: explanations for the temperature–
858 size rule with special emphasis on the role of oxygen. *Biological Reviews*, 96(1), 247–268.
859 <https://doi.org/10.1111/brv.12653>

860 Véron, M., Duhamel, E., Bertignac, M., Pawlowski, L., & Huret, M. (2020). Major changes
861 in sardine growth and body condition in the Bay of Biscay between 2003 and 2016:
862 Temporal trends and drivers. *Progress in Oceanography*, 182, 102274.
863 <https://doi.org/10.1016/j.pocean.2020.102274>

864 Ward, B. A., Dutkiewicz, S., Jahn, O., & Follows, M. J. (2012). A size-structured food-web
865 model for the global ocean. *Limnology and Oceanography*, 57(6), 1877–1891.
866 <https://doi.org/10.4319/lo.2012.57.6.1877>

867 Wootton, H.F., Morrongiello, J.R., Schmitt, T., Audzijonyte, A., 2022. Smaller adult fish
868 size in warmer water is not explained by elevated metabolism. *Ecol Lett* 25, 1177–1188.
869 <https://doi.org/10.1111/ele.13989>

870 Zarubin, M., Farstey, V., Wold, A., Falk-Petersen, S., & Genin, A. (2014). Intraspecific
871 differences in lipid content of calanoid copepods across fine-scale depth ranges within
872 the photic layer. *PLoS ONE*, 9(3), 1–10. <https://doi.org/10.1371/journal.pone.0092935>

873 Zhang, Y., Claireaux, G., Takle, H., Jørgensen, S. M., & Farrell, A. P. (2018). A three-phase
874 excess post-exercise oxygen consumption in Atlantic salmon *Salmo salar* and its response
875 to exercise training. *Journal of Fish Biology*, 92(5), 1385–1403.
876 <https://doi.org/10.1111/JFB.13593>

877 Zuur, A.F., Ieno, E.N., Walker, N., Saveliev, A.A., Smith, G.M., 2009. Mixed effects models
878 and extensions in ecology with R, Statistics for Biology and Health. Springer New York,
879 New York, NY. <https://doi.org/10.1007/978-0-387-87458-6>

880

881

Supplementary material

882

883

884 **Material and methods**

885 Each respirometer was shaped by a vertical PVC pipe and included three perforated semi-cylinders of
886 PVC pipe in its interior section (Fig. S2). An external pump was connected to this system to collect
887 water from one semi-cylinder and deliver it to the two other semi-cylinders, so water was constantly
888 mixed in the respirometer (yellow arrows in Fig. S2). Outside of measurement period, respirometer
889 water was renewed with water pumped from continuously aerated buffer tanks (300 L) into the same
890 hemispheres that the external pump to maintain dissolved O₂ concentrations close to saturation (i.e.
891 100 %)(white arrows in Fig. S2). Excess of water was collected through a PVC pipe and returned to its
892 given buffer tanks. These buffer tanks were supplied with the same seawater and the temperatures
893 were maintained equal to either 16°C (cool) or 21°C (warm), maintaining constant temperature in
894 respirometers. Pumps in buffer tanks were controlled by an electrical timer and were turned off during
895 measurements and water level settled at the overflow to provide a constant volume (50 L). Large buffer
896 tanks were continuously supplied with water pumped from the sea, filtered through sand filter (30–40
897 µm) and sterilized with UV light. The photoperiod was adjusted to 12-12h cycle.

898

899

900

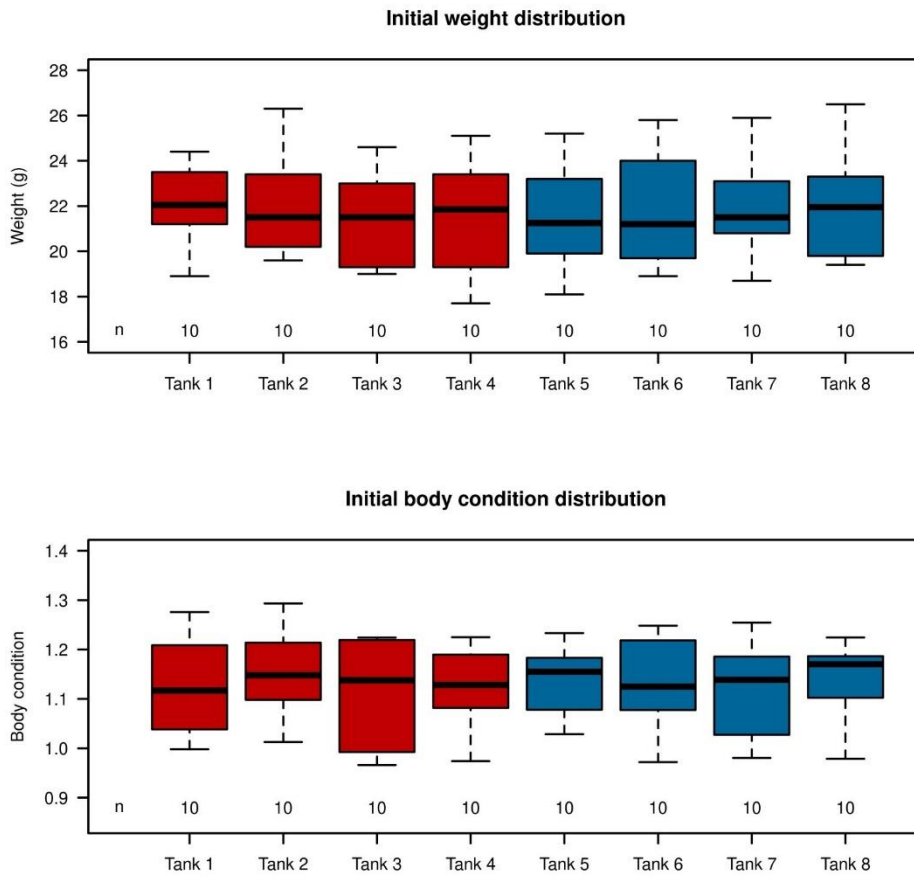
901

902

903

904

905 **Figures**



906

907

908 Fig. S1: Distribution of body mass (A) and condition (B) of sardines for each tank at the beginning of the experiment.

909 Colors refer to the water temperature in each tank i.e. either 21°C (in red) or 16°C (in blue). The number of

910 individuals is given by n at the bottom of the panels.

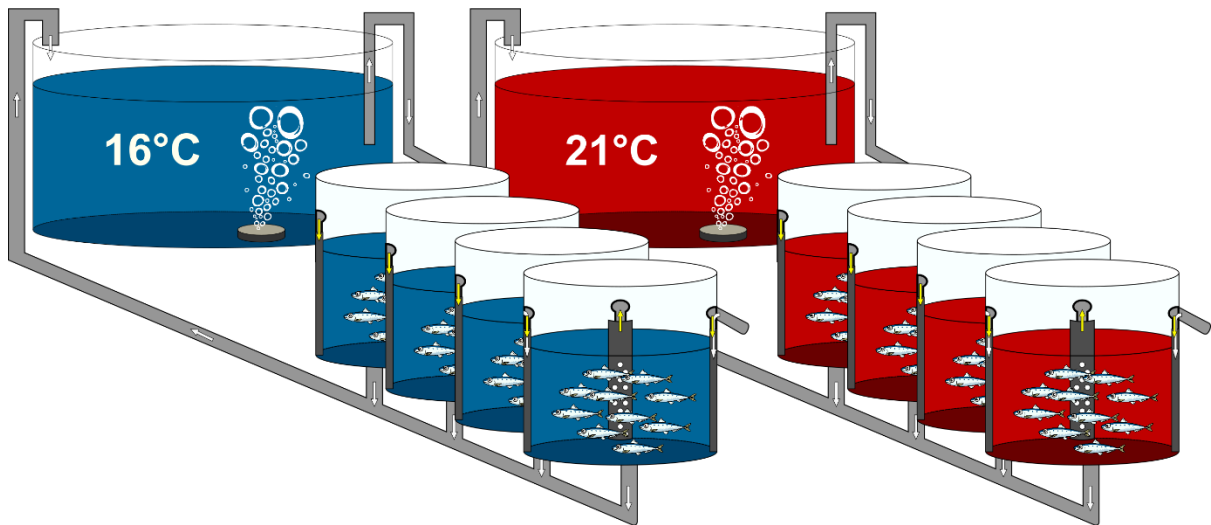
911

912

913

914

915



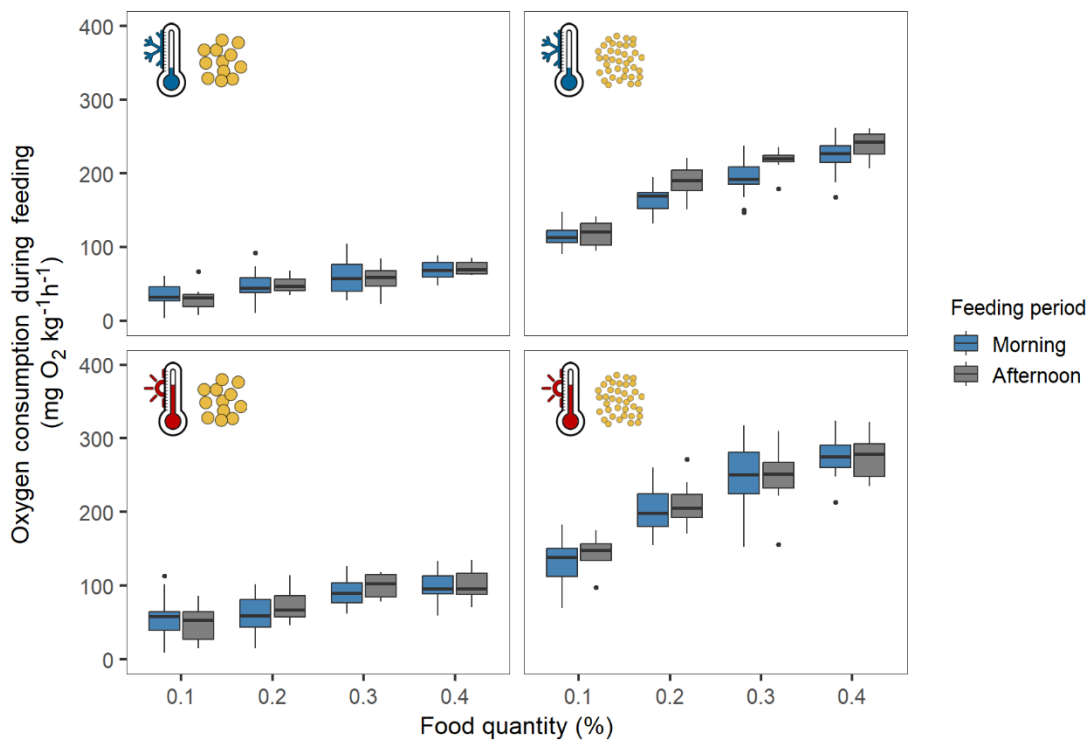
916

917

918 *Fig. S2: The entire setup was composed by (i) 2 large aerated buffer tanks that homogenized water quality between*
919 *tanks and maintained constant water temperature over time and (ii) 8 small experimental tanks. Each 50L*
920 *experimental tank, in which 10 individuals were reared, was modified as automated respirometer with a continuous*
921 *water flow that ensured the homogeneity of the water parameters (indicated by yellow arrows). The renewal and*
922 *excess water flows are indicated by white arrows. The two colors refer to the two water temperatures: 21°C in red*
923 *and 16°C in blue.*

924

925

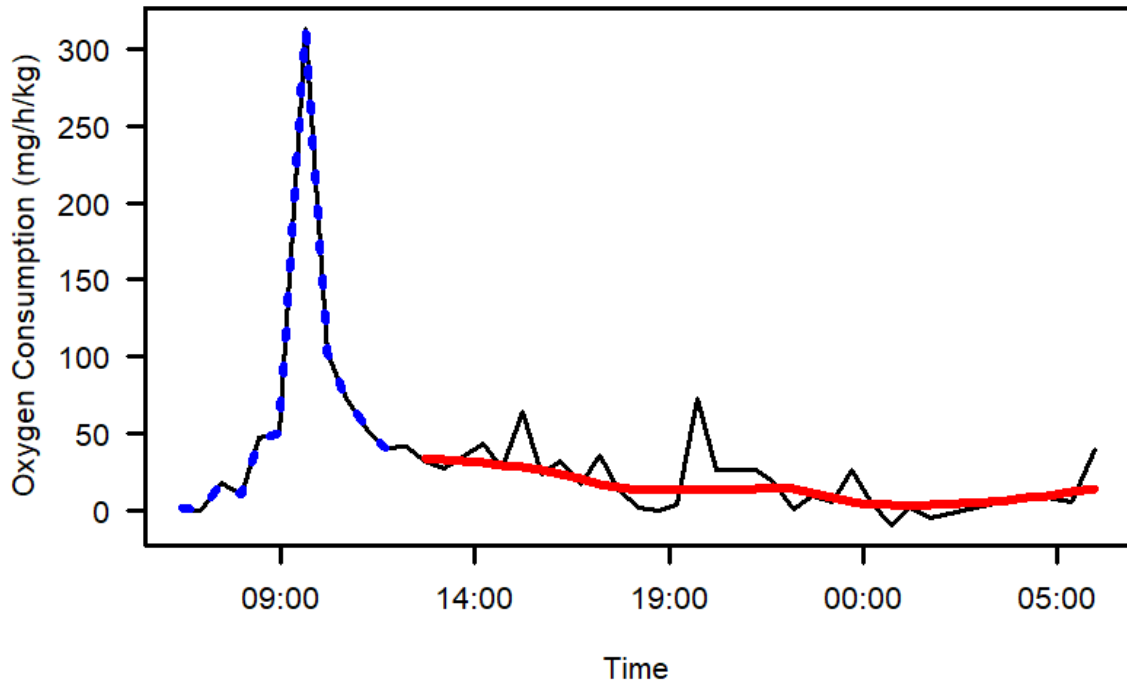


927

928

929 *Fig. S3: Boxplots of oxygen consumption during the 1st meal in the morning (in blue) and the 2nd meal in the*
 930 *afternoon (in grey) for the four feeding treatment x temperature (cool temperature and large particles, cool*
 931 *temperature and small particles, warm temperature and large particles and warm temperature and small particles).*
 932 *Oxygen consumptions have been calculated relative to a control baseline that was estimated as the mean of the*
 933 *preceding 2.5 hours. This calculation avoided bias when lights were turned on 1.5 hour before the 1st daily meal,*
 934 *and also potential remnant effects of digestion of that 1st meal for the 2nd meal period. No significant effect of the*
 935 *period (morning vs. afternoon) on the oxygen consumption over feeding treatment x temperature was found*
 936 *(ANOVA, $p = 0.63$).*

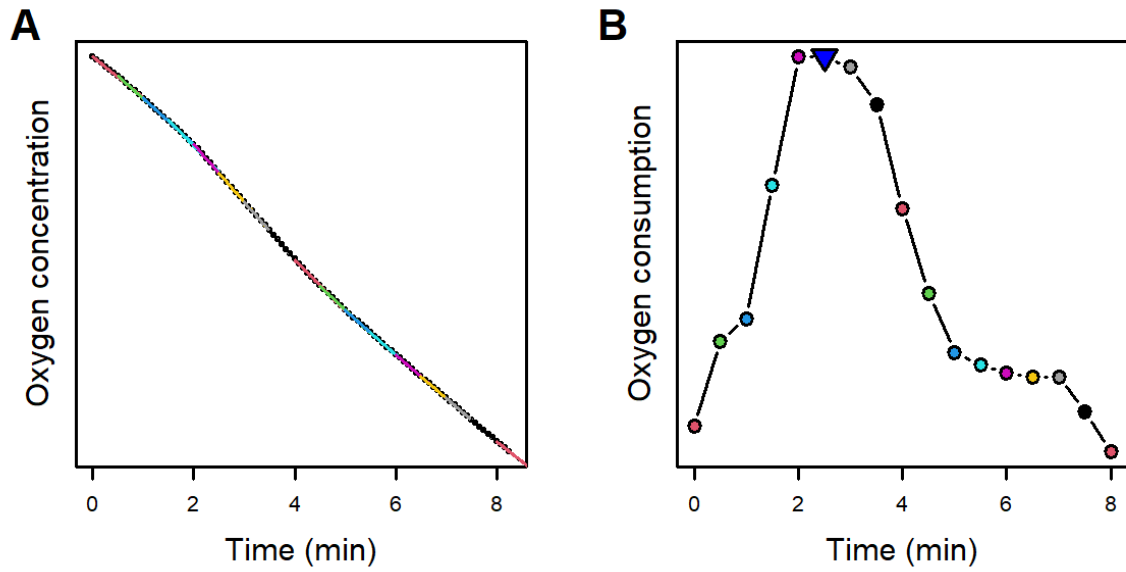
937
938



939
940
941
942
943
944
945

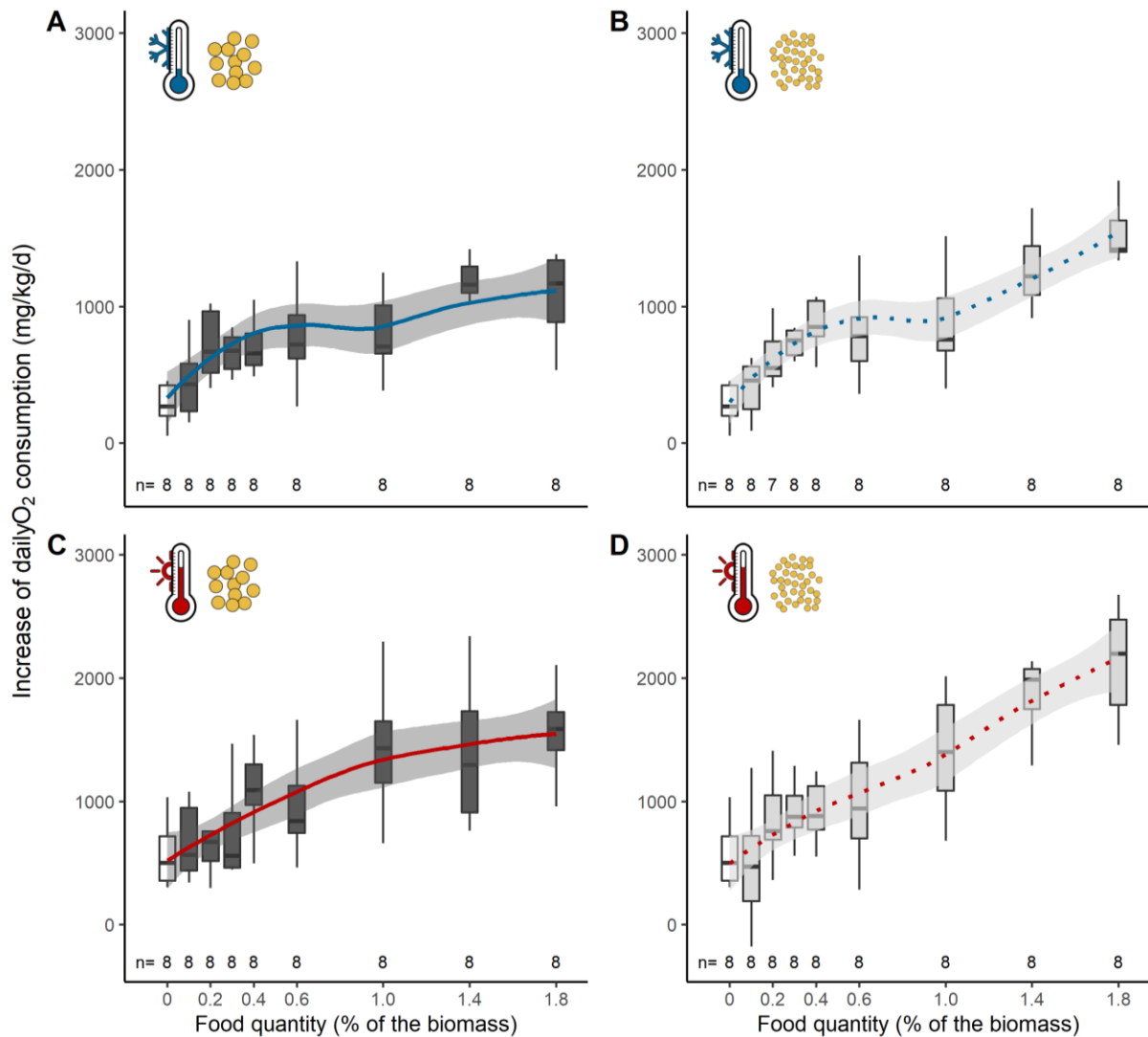
Fig. S4: Oxygen consumption over time from 06:00 a.m. and for 24 hours. The black line represents the original data of the oxygen consumption. The estimation of the daily oxygen consumption was calculated over a combination of two periods: (1) following original data from 06:00 a.m. until noon to catch the peak of oxygen consumption observed during the meal period (dashed blue line) and (2) smoothed values of the oxygen consumption after noon to avoid any outlier (e.g. peak at 19:30) that could distort daily consumption estimation (solid red line).

946
947
948



949
950
951
952
953
954

Fig. S5: Smoothed oxygen concentration (A) and oxygen consumption (B) after the start of the meal. Oxygen consumptions were estimated every 30 seconds using linear regressions over 1 minute on smoothed oxygen concentrations (lines in A and corresponding points in B). The blue triangle represents the maximal oxygen consumption reached during the meal.

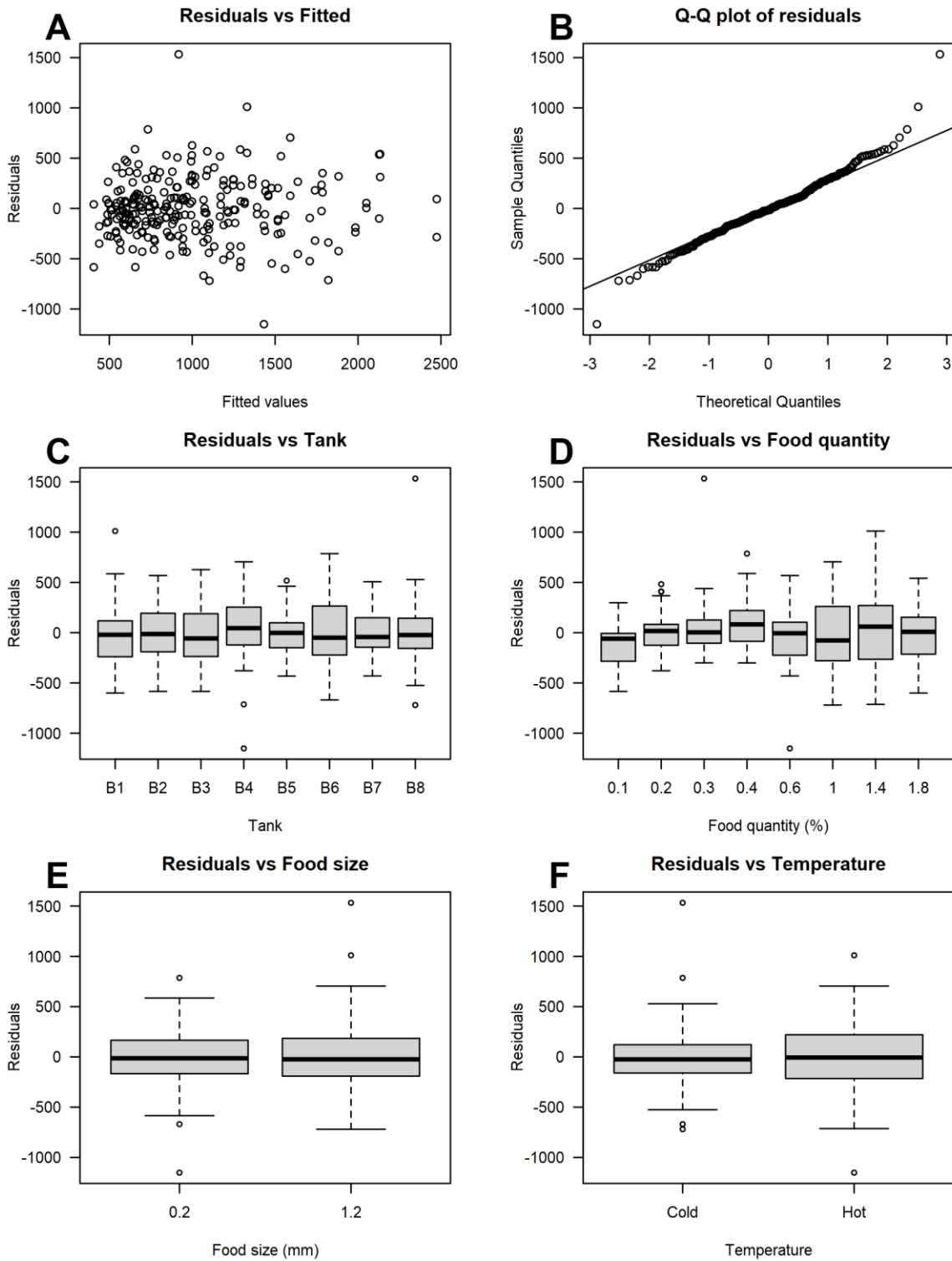


956

957

958 *Fig. S6: Boxplot of the daily oxygen consumption increase (relative to basal oxygen consumption and due to*
 959 *movement, food foraging and digestion) according to the food ration for the 4 experimental treatments: cool*
 960 *temperature and large particles (A), cool temperature and small particles (B), warm temperature and large particles*
 961 *(C) warm temperature and small particles (D). Dotted (for small particles) and solid lines (for large particles)*
 962 *represent the smooth increase of the median daily oxygen uptake in relation to the food ration. Grey bands*
 963 *represent 95% confidence intervals of smooth increases. White colour represents data during days of fasting, while*
 964 *light and dark grey represent small and large particles, respectively. Blue and red colours represent cool (16°C)*
 965 *and warm (21°C) temperatures, respectively. Only slopes (i.e. oxygen consumption) with R squared ≥ 0.95 were*
 966 *used. Sample size (i.e. number of days) is given as 'n' at the bottom of each panel. Outliers were removed for*
 967 *clarity purpose.*

968



969

970

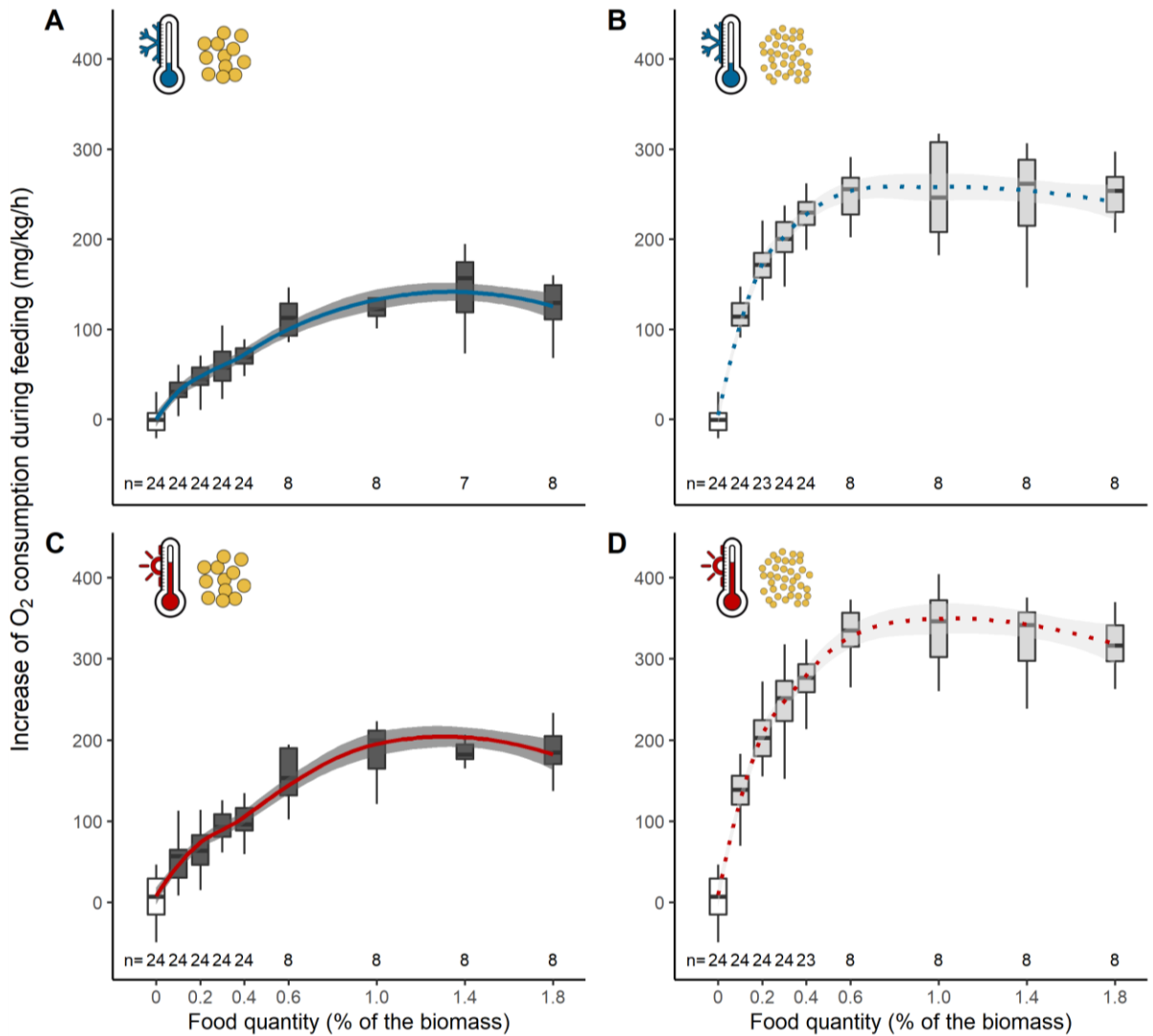
971 *Fig. S7: Diagnostic plots of the selected model for the daily oxygen consumption. A: Fitted values versus residuals.*

972 *B: Q-Q plot of the residuals. C: Residuals versus Tank ID. D: Residuals versus Food ration. E: Residuals versus*

973 *Food size. F: Residuals versus Temperature.*

974

B Meal period

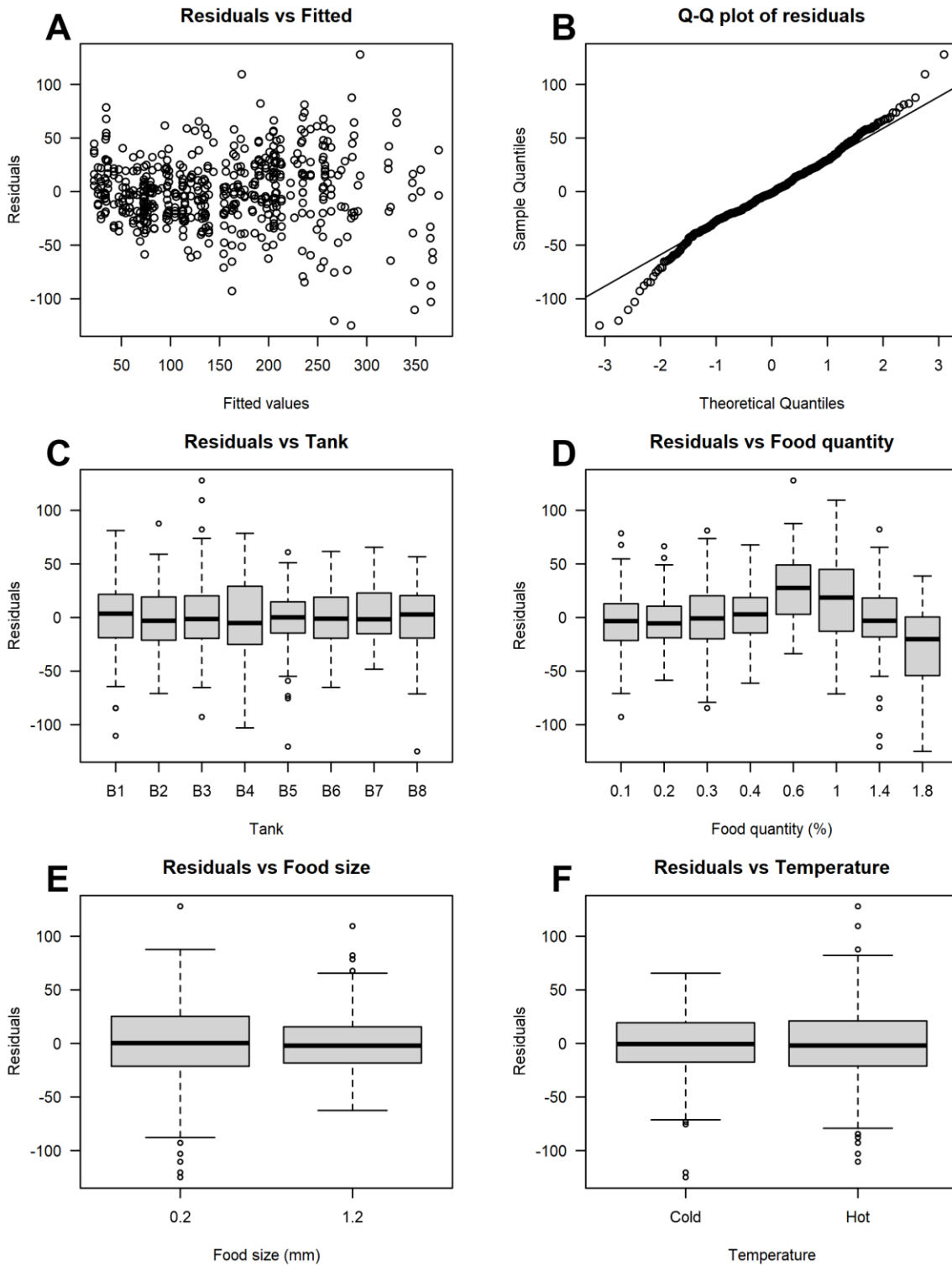


975

976

977 *Fig. S8: Boxplot of the oxygen consumption increase during feeding (relative to the previous 2.5h oxygen*
 978 *consumption) according to the food ration for the 4 experimental treatments: cool temperature and large particles*
 979 *(A), cool temperature and small particles (B), warm temperature and large particles (C) warm temperature and*
 980 *small particles (D). Dotted (for small particles) and solid lines (for large particles) represent the smooth increase of*
 981 *the median daily oxygen uptake in relation to the food ration. Grey bands represent 95% confidence intervals of*
 982 *smooth increases. White colour represents data during days of fasting, while light and dark grey represent small*
 983 *and large particles, respectively. Blue and red colours represent cool (16°C) and warm (21°C) temperatures,*
 984 *respectively. Only slopes (i.e. oxygen consumption) with R squared ≥ 0.95 were used. Sample size (i.e. number of*
 985 *meals) is given as 'n' at the bottom of each panel. Sample size is greater for food ration below 0.6% because*
 986 *results from experiments 1 and 2 are gathered here (n = 8 and n = 16 for experiment 1 and experiment 2,*
 987 *respectively). Outliers were removed for clarity purpose.*

988



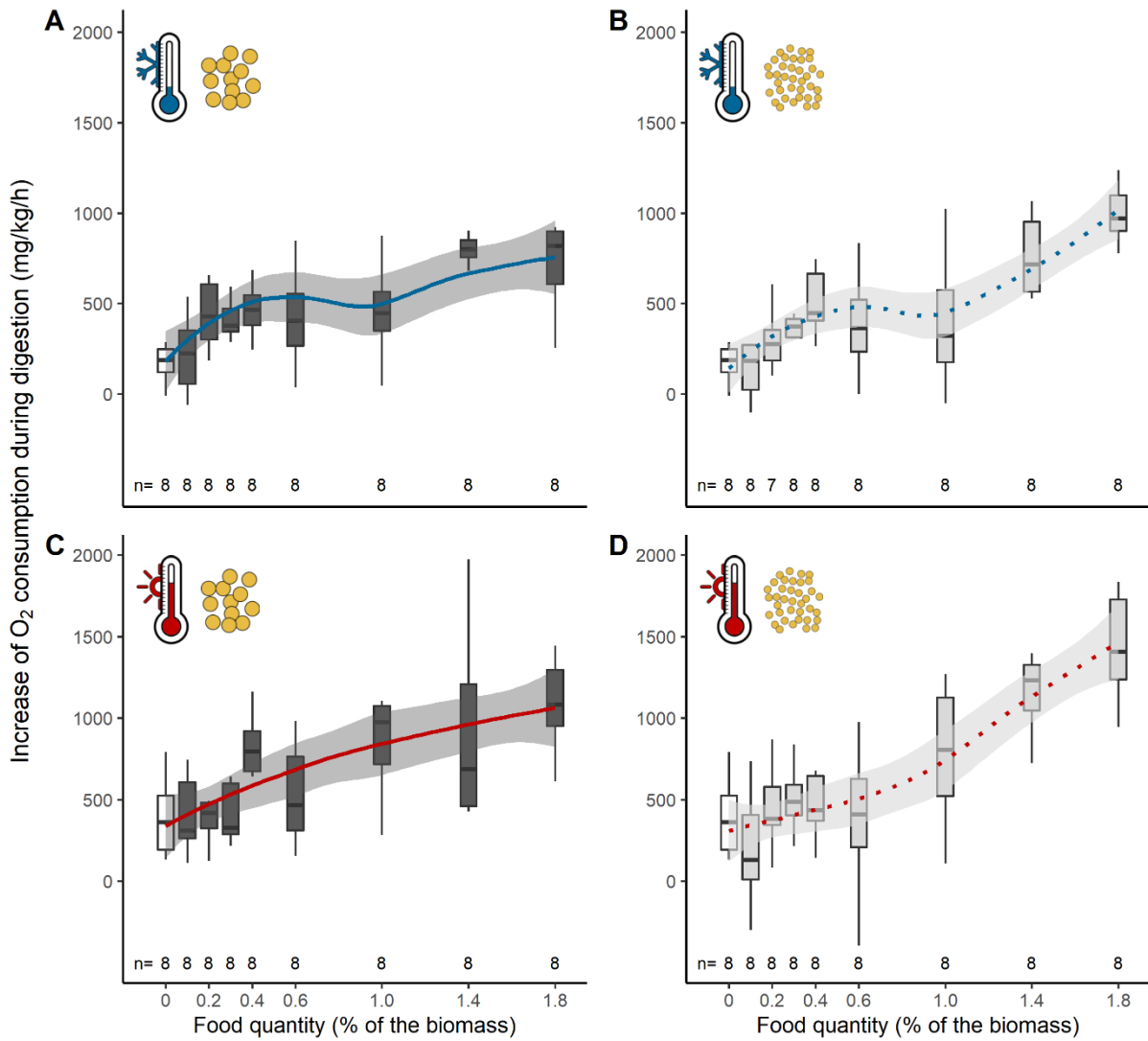
989

990

991 *Fig. S9: Diagnostic plots of the selected model for the oxygen consumption during feeding. A: Fitted values versus*
 992 *residuals. B: Q-Q plot of the residuals. C: Residuals versus Tank ID. D: Residuals versus Food ration. E: Residuals*
 993 *versus Food size. F: Residuals versus Temperature.*

994

C Digestion

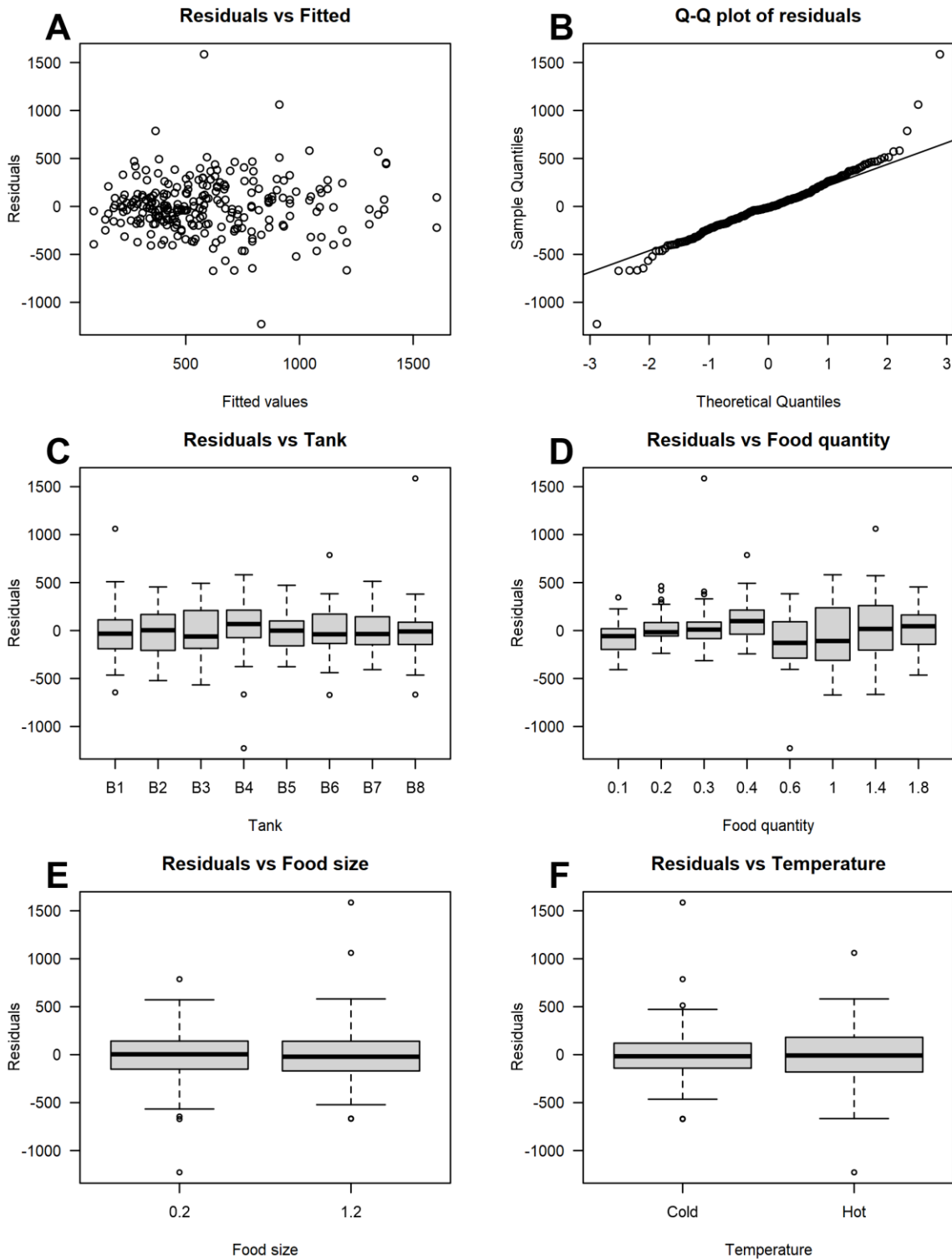


995

996

997 *Fig. S10: Boxplot of the oxygen consumption increase (relative to basal oxygen consumption) during the digestion*
 998 *(here 1.5 hour after the beginning of the meal period) according to the food ration for the 4 experimental treatments:*
 999 *cool temperature and small particles (A), cool temperature and large particles (B), warm temperature and small*
 1000 *particles (C) warm temperature and large particles (D). Dotted (for small particles) and solid lines (for large*
 1001 *particles) represent the increase of the median oxygen uptake during digestion in relation to the food ration. Grey*
 1002 *bands represent 95% confidence intervals of smooth increases. White color represents data during days of fasting,*
 1003 *while light and dark grey represent small and large particles, respectively. Blue and red colors represent cool (16°C)*
 1004 *and warm (21°C) temperature, respectively. Sample size (i.e. number of meals) is given as 'n' at the bottom of*
 1005 *each panel.*

1006



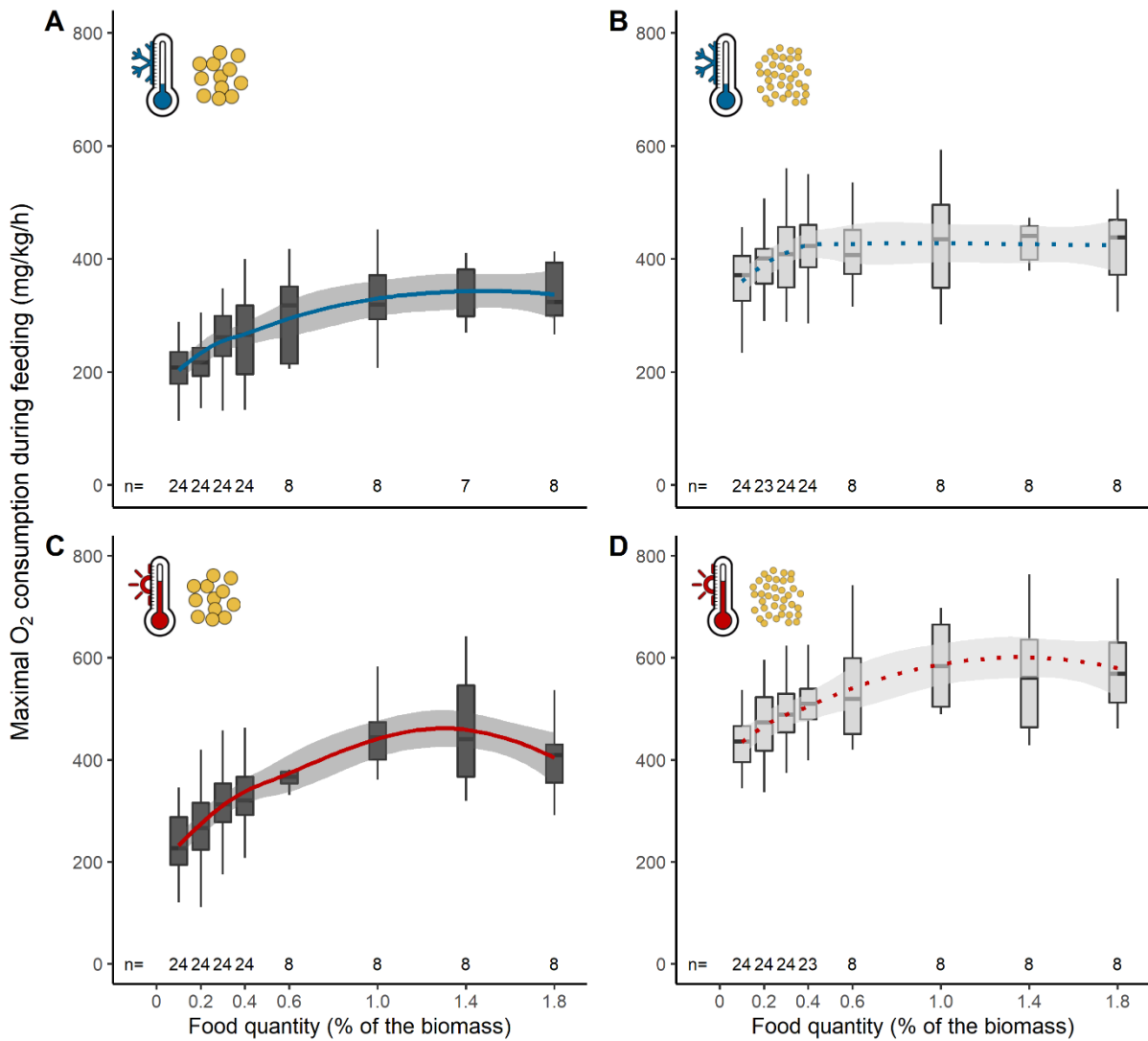
1007

1008

1009 *Fig. S11: Diagnostic plots of the selected model for the oxygen consumption during digestion. A: Fitted values*
 1010 *versus residuals. B: Q-Q plot of the residuals. C: Residuals versus Tank ID. D: Residuals versus Food ration. E:*
 1011 *Residuals versus Food size. F: Residuals versus Temperature.*

1012

D Maximum

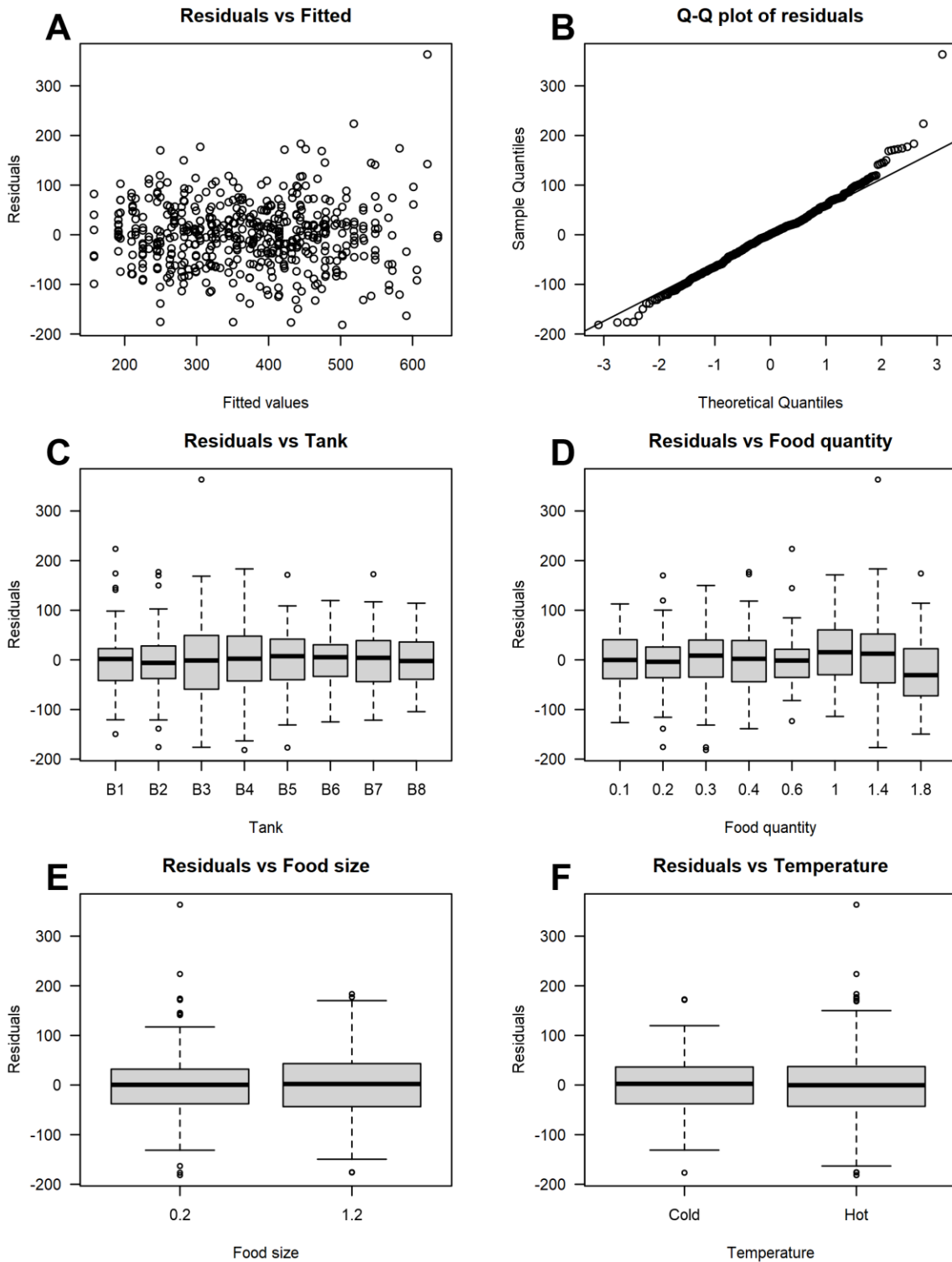


1013

1014

1015 *Fig. S12: Boxplot of the maximal oxygen consumption increase (relative to basal oxygen consumption) during the*
 1016 *meal period according to the food ration for the 4 experimental treatments: cool temperature and small particles*
 1017 *(A), cool temperature and large particles (B), warm temperature and small particles (C) warm temperature and*
 1018 *large particles (D). Dotted (for small particles) and solid lines (for large particles) represent the increase of the*
 1019 *median of the maximal oxygen uptake on relation to the food ration. Light and dark grey represent small and large*
 1020 *particles, respectively. Grey bands represent 95% confidence intervals of smooth increases. Blue and red colors*
 1021 *represent cool (16°C) and warm (21°C) temperature, respectively. Sample size (i.e. number of meals) is given as*
 1022 *'n' at the bottom of each panel. Sample size is greater for the 4 smallest quantities (i.e. 0.1, 0.2, 0.3 and 0.4%)*
 1023 *because oxygen consumption obtained from experiments 1 and 2 were pooled here.*

1024



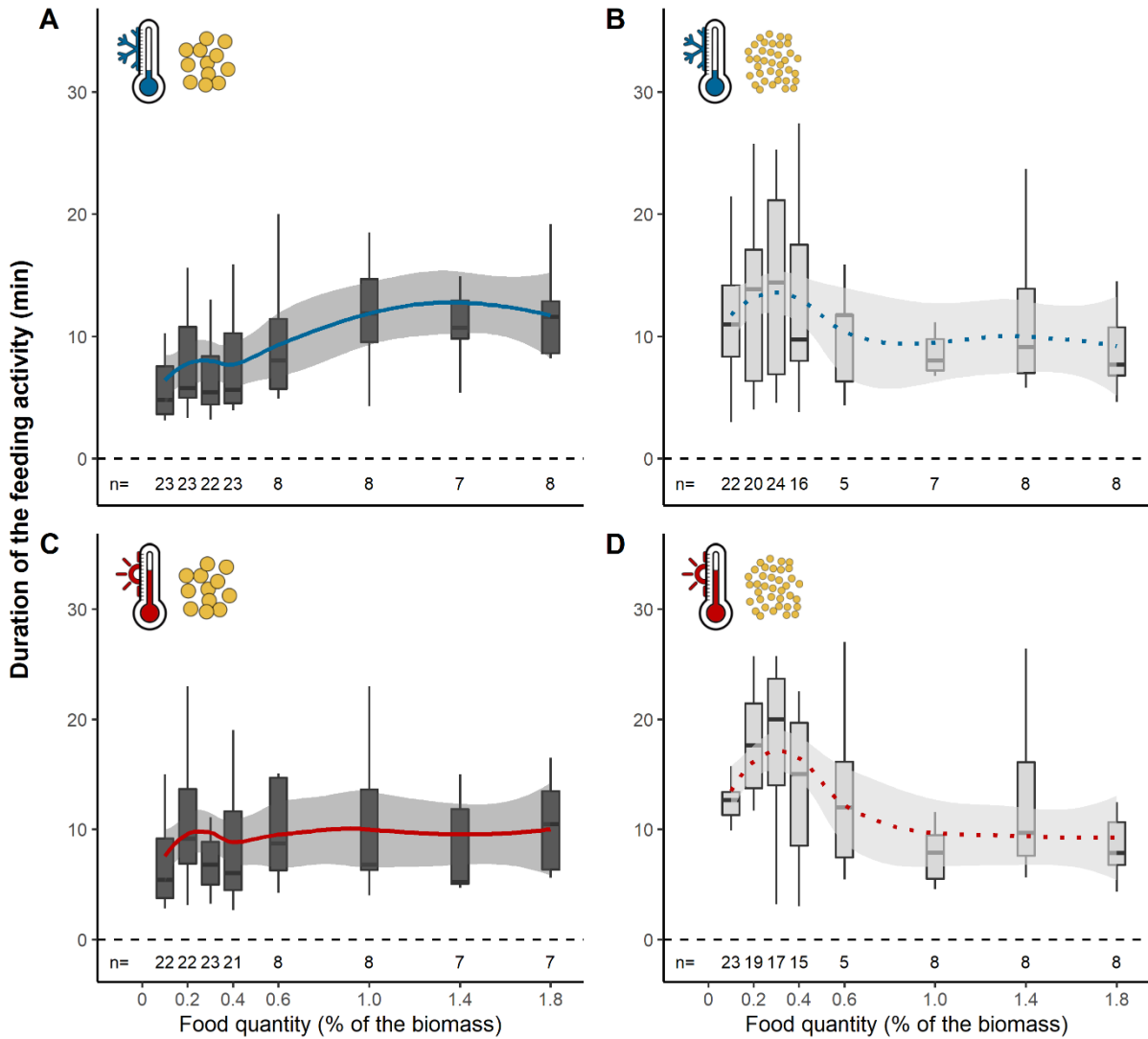
1025

1026

1027 *Fig. S13: Diagnostic plots of the selected model for the maximum oxygen consumption during feeding. A: Fitted*
 1028 *values versus residuals. B: Q-Q plot of the residuals. C: Residuals versus Tank ID. D: Residuals versus Food*
 1029 *ration. E: Residuals versus Food size. F: Residuals versus Temperature.*

1030

E Feeding duration

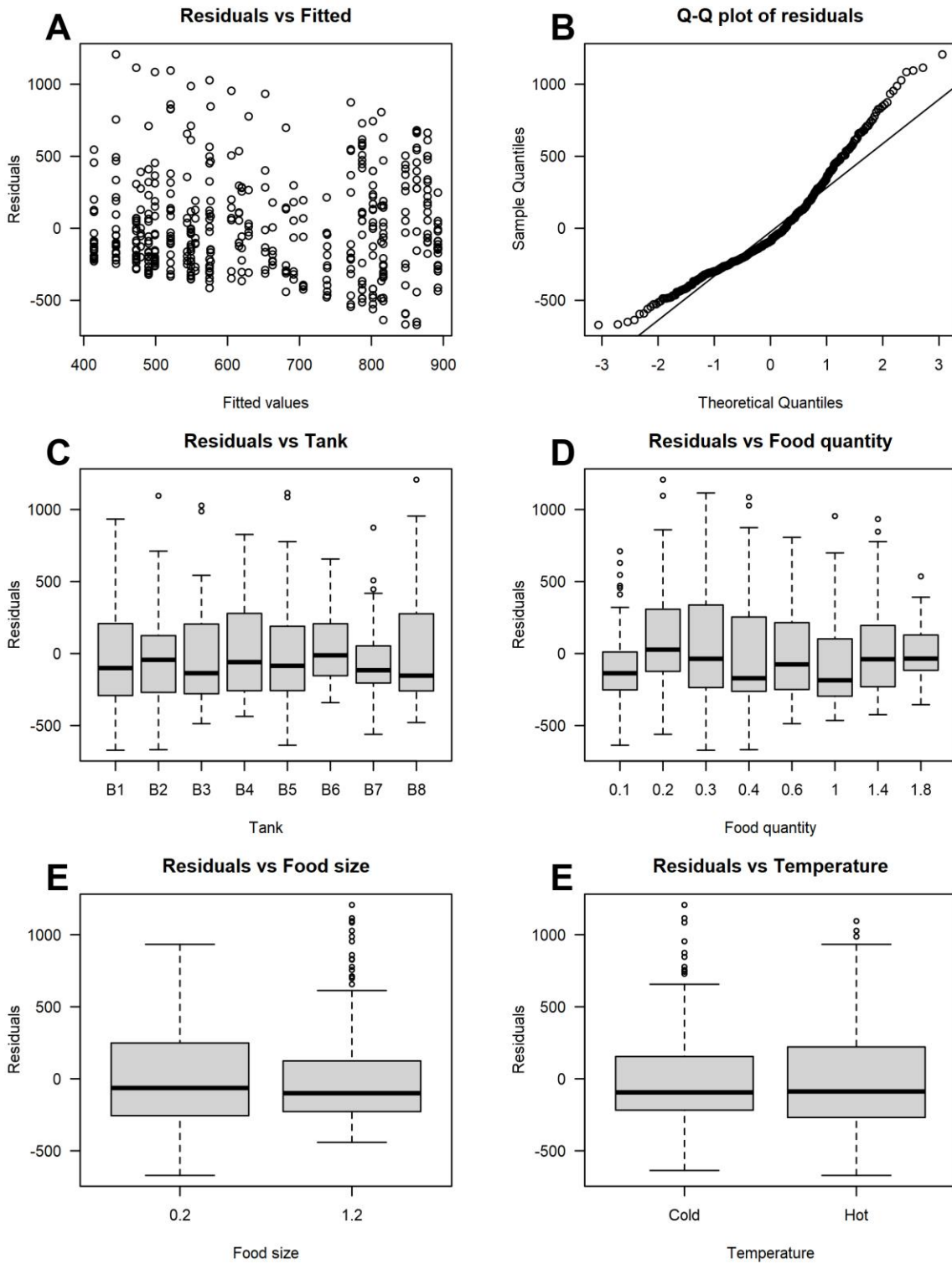


1031

1032

1033 *Fig. S14: Boxplot of the feeding duration according to the food ration for the 4 experimental treatments: cool*
 1034 *temperature and small particles (A), cool temperature and large particles (B), warm temperature and small particles*
 1035 *(C) warm temperature and large particles (D). Dotted (for small particles) and solid lines (for large particles)*
 1036 *represent the variations of the median feeding duration on relation to the food ration. Grey bands represent 95%*
 1037 *confidence intervals of smooth increases. Light and dark grey represent small and large particles, respectively.*
 1038 *Blue and red colors represent cool (16°C) and warm (21°C) temperature, respectively. Sample size (i.e. number of*
 1039 *meals) is given as 'n' at the bottom of each panel. Sample size is greater for the 4 smallest quantities (i.e. 0.1, 0.2,*
 1040 *0.3 and 0.4%) because oxygen consumption obtained from experiments 1 and 2 were pooled here. When a feeding*
 1041 *duration could not be calculated (e.g. no breakpoint), data was removed from this analysis.*

1042



1043

1044 *Fig. S15: Diagnostic plots of the selected model for the feeding duration. A: Fitted values versus residuals. B: Q-Q*
 1045 *plot of the residuals. C: Residuals versus Tank ID. D: Residuals versus Food ration. E: Residuals versus Food*
 1046 *size.*

1047 **Tables**

1048

1049 *Table S1: Results of model selection on the daily oxygen consumption (df, logLik, AICc and ΔAICc).*

1050 *The best-fitting model was selected based on the lowest AICc values (Burnham and Anderson, 2002)*

1051 *following Zuur et al. 2003. When difference in AICc (ΔAICc) was lower than two between these models,*

1052 *the more parsimonious model was selected (Burnham and Anderson, 2002). The selected models is*

1053 *represented in bold.*

1054

Models	df	logLik	AICc	ΔAICc
~ Food ration x Temperature + Food ration x Food size	8	-1837.9	3692.3	0.0
~ Food ration x Temperature + Temperature x Food size + Food ration x Food size	9	-1837.7	3694.2	1.8
~ Food ration x Food size x Temperature	10	-1837.2	3695.4	3.1
~ Food ration x Temperature + Food size	7	-1846.9	3708.2	15.9
~ Food ration x Food size + Temperature	7	-1847.7	3709.8	17.5
~ Food ration x Temperature + Temperature x Food size	8	-1846.7	3710.1	17.8
~ Food ration x Food size	6	-1849.2	3710.7	18.4
~ Food ration x Food size + Temperature x Food size	8	-1847.5	3711.6	19.3
~ Food ration x Temperature	6	-1850.3	3713.0	20.7
~ Food ration + Food size + Temperature	6	-1856.1	3724.5	32.2
~ Food ration + Food size	5	-1857.6	3725.4	33.1
~ Food ration + Food size x Temperature	7	-1855.9	3726.4	34.0
~ Food ration + Temperature	5	-1859.3	3728.8	36.4
~ Food ration	4	-1860.8	3729.7	37.4
~ Food size + Temperature	5	-1939.6	3889.4	197.1
~ Food size	4	-1941.0	3890.2	197.9
~ Temperature	4	-1941.3	3890.7	198.4
~ Food size x Temperature	6	-1939.5	3891.4	199.1
~ 1	3	-1942.7	3891.6	199.3

1055

1056

1057 *Table S2: Results of the selected mixed effect model on the daily oxygen consumption (Estimates, 95%*
 1058 *confidence intervals and p-values). Estimations of the predictors of all other fixed effects were based*
 1059 *on the estimations of treatment 'warm temperature and small particles'. The selected model is*
 1060 *presented using REML estimation.*

1061



















Fixed effects:			
<i>Predictors</i>	<i>Estimates</i>	<i>95% CI</i>	<i>p-value</i>
(Intercept)	555.39	313.23 – 797.54	<0.001
Food ration	868.58	751.42 – 985.74	<0.001
Food size [Large]	106.34	-19.32 – 232.00	0.097
Temperature [Cool]	-41.06	-371.97 – 289.84	0.807
Food size [Large] x Food ration	-294.84	-430.28 – -159.40	<0.001
Temperature [Cool] x Food ration	-308.42	-443.85 – -172.98	<0.001
Random Effects:			
σ^2	100091.73		
$\tau_{00 \text{ Tank}}$	48311.87		
ICC	0.33		
N_{Tank}	8		
Observations	255		
Marginal R^2 / Conditional R^2	0.490 / 0.656		

1062

1063

1064 *Table S3: Results of linear mixed-effects models on the daily, while feeding, while digesting, maximal*
 1065 *oxygen consumptions (relative to basal oxygen consumption, see details in Material and Methods) and*
 1066 *feeding duration according to the food ration for food size and temperature. Slopes were provided after*
 1067 *being back-transformed for models on feeding and maximal oxygen consumptions. Slopes are given in*
 1068 *mgO₂/kg/d for daily MO₂ and during digestion, in mgO₂/kg/h for oxygen consumption during feeding*
 1069 *and maximal MO₂, and in min for feeding duration.*

1070

Period	Treatment	Slope	[95% CI]
Daily	 Large particles	420	[324;515]
	 Small particles	714	[618;810]
	 At 16°C	413	[317;509]
	 At 21°C	721	[626;817]
Meal period	 Large particles	95	[85;105]
	 Small particles	129	[119;139]
	 At 16°C	91	[81;101]
	 At 21°C	133	[123;143]
Digestion	 Large particles	300	[213;388]
	 Small particles	533	[445;621]
	 At 16°C	306	[218;394]
	 At 21°C	527	[439;615]
Maximal	 Large particles	132	[113;152]
	 Small particles	87	[67;106]
	 At 16°C	78	[58;97]
	 At 21°C	141	[122;161]
Duration	 Large particles	4	[1;7]
	 Small particles	-3	[-6;0]

1071

1072 *Table S4: Results of model selection on the oxygen consumption during feeding (df, logLik, AICc and*
 1073 *ΔAICc). The best-fitting model was selected based on the lowest AICc values (Burnham and Anderson,*
 1074 *2002) following Zuur et al. 2003. When difference in AICc (ΔAICc) was lower than two between these*
 1075 *models, the more parsimonious model was selected (Burnham and Anderson, 2002). The selected*
 1076 *models is represented in bold. Food ration was log-transformed for model selection.*

1077

Models	df	logLik	AICc	ΔAICc
~ log(Food ration) x Food size x Temperature	10	-2505.3	5031.0	0.0
~ log(Food ration) x Temperature + Temperature x Food size + log(Food ration) x Food size	9	-2506.4	5031.1	0.1
~ log(Food ration) x Temperature + log(Food ration) x Food size	8	-2509.3	5035.0	4.0
~ log(Food ration) x Temperature + Temperature x Food size	8	-2517.4	5051.1	20.1
~ log(Food ration) x Temperature + Food size	7	-2520.3	5054.8	23.7
~ log(Food ration) x Food size + Temperature x Food size	8	-2523.3	5062.9	31.9
~ log(Food ration) x Food size + Temperature	7	-2526.1	5066.5	35.5
~ log(Food ration) + Food size x Temperature	7	-2533.5	5081.2	50.2
~ log(Food ration) + Food size + Temperature	6	-2536.2	5084.6	53.6
~ log(Food ration) x Food size	6	-2536.3	5084.7	53.7
~ log(Food ration) + Food size	5	-2546.4	5102.9	71.8
~ Food size + Temperature	5	-2794.5	5599	568.0
~ Food size x Temperature	6	-2793.6	5599.4	568.3
~ Food size	4	-2804.3	5616.8	585.7
~ log(Food ration) x Temperature	6	-2917.4	5847.0	815.9
~ log(Food ration) + Temperature	5	-2920.6	5851.2	820.2
~ log(Food ration)	4	-2929.2	5866.5	835.5
~ Temperature	4	-3004.7	6017.6	986.5
~ 1	3	-3012.6	6031.3	1000.3

1078

1079

1080

1081 *Table S5: Results of the selected mixed effect model on the oxygen consumption during feeding*
 1082 *(Estimates, 95% confidence intervals and p-values). Estimations of the predictors of all other fixed*
 1083 *effects were based on the estimations of treatment ‘warm temperature and small particles’. The selected*
 1084 *model is presented using REML estimation. Food ration was log-transformed before regression.*

1085

Fixed effects:			
<i>Predictors</i>	<i>Estimates</i>	<i>95% CI</i>	<i>p-value</i>
(Intercept)	324.08	314.62 – 334.98	<0.001
log(Food ration)	72.58	67.01 – 78.72	<0.001
Food size [Large]	-156.87	-168.88 – -146.69	<0.001
Temperature [Cool]	-70.01	-83.52 – -56.74	<0.001
log(Food ration) x Food size [Large]	-15.81	-23.06 – -9.52	<0.001
log(Food ration) x Temperature [Cool]	-20.29	-27.06 – -13.52	<0.001
Food size [Large] x Temperature [Cool]	14.05	2.76 – 25.94	0.015
Random Effects:			
σ^2	1106.87		
τ_{00} Tank	29.07		
ICC	0.03		
N_{Tank}	8		
Observations	509		
Marginal R ² / Conditional R ²	0.863 / 0.867		

1086

1087

1088

1089

1090 *Table S6: Results of model selection on the oxygen consumption during digestion (df, logLik, AICc and*
 1091 *ΔAICc). The best-fitting model was selected based on the lowest AICc values (Burnham and Anderson,*
 1092 *2002) following Zuur et al. 2003. When difference in AICc (ΔAICc) was lower than two between these*
 1093 *models, the more parsimonious model was selected (Burnham and Anderson, 2002). The selected*
 1094 *models is represented in bold.*

1095

Models	df	logLik	AICc	ΔAICc
~ Food ration x Temperature + Food ration x Food size	8	-1813.3	3643.1	0.0
~ Food ration x Temperature + Temperature x Food size + Food ration x Food size	9	-1813.3	3645.3	2.1
~ Food ration x Food size x Temperature	10	-1812.7	3646.3	3.2
~ Food ration x Temperature	6	-1820.1	3652.6	9.5
~ Food ration x Food size + Temperature	7	-1819.4	3653.2	10.1
~ Food ration x Food size	6	-1820.8	3653.9	10.8
~ Food ration x Temperature + Food size	7	-1820.0	3654.5	11.4
~ Food ration x Food size + Temperature x Food size	8	-1819.4	3655.3	12.2
~ Food ration x Temperature + Temperature x Food size	8	-1820.0	3656.6	13.5
~ Food ration + Temperature	5	-1826.0	3662.2	19.1
~ Food ration	4	-1827.3	3662.9	19.7
~ Food ration + Food size + Temperature	6	-1825.8	3664.0	20.9
~ Food ration + Food size	5	-1827.2	3664.7	21.6
~ Food ration + Food size x Temperature	7	-1825.8	3666.1	23.0
~ Temperature	4	-1887.8	3783.8	140.7
~ 1	3	-1889.2	3784.4	141.3
~ Food size + Temperature	5	-1887.8	3785.8	142.7
~ Food size	4	-1889.1	3786.4	143.3
~ Food size x Temperature	6	-1887.8	3787.9	144.8

1096

1097

1098 *Table S7: Results of the selected mixed effect model on the oxygen consumption during digestion*
 1099 *(Estimates, 95% confidence intervals and p-values). Estimations of the predictors of all other fixed*
 1100 *effects were based on the estimations of treatment ‘warm temperature and small particles’. The selected*
 1101 *model is presented using REML estimation.*

1102

Fixed effects:			
<i>Predictors</i>	<i>Estimates</i>	<i>95% CI</i>	<i>p-value</i>
(Intercept)	212.24	33.29 – 391.20	0.020
Food ration	643.27	536.00 – 750.54	<0.001
Food size [Large]	187.13	72.08 – 302.18	0.002
Temperature [Cool]	-17.63	-257.48 – 222.22	0.885
Food ration x Food size [Large]	-232.56	-356.57 – -108.56	<0.001
Food ration x Temperature [Cool]	-221.02	-345.02 – -97.01	0.001
Random Effects:			
σ^2	83904.80		
$\tau_{00 \text{ Tank}}$	22833.11		
ICC	0.21		
N_{Tank}	8		
Observations	255		
Marginal R^2 / Conditional R^2	0.410 / 0.536		

1103

1104 *Table S8: Results of model selection on the maximal oxygen consumption during feeding (df, logLik,*
 1105 *AICc and Δ AICc). The best-fitting model was selected based on the lowest AICc values (Burnham and*
 1106 *Anderson, 2002) following Zuur et al. 2003. When difference in AICc (Δ AICc) was lower than two*
 1107 *between these models, the more parsimonious model was selected (Burnham and Anderson, 2002).*
 1108 *The selected models is represented in bold. Food ration was log-transformed for model selection.*

1109

Models	df	logLik	AICc	Δ AICc
~ log(Food ration) x Temperature + Temperature x Food size + log(Food ration) x Food size	9	-2865.6	5749.5	0.0
~ log(Food ration) x Food size x Temperature	10	-2865.4	5751.3	1.7
~ log(Food ration) x Temperature + log(Food ration) x Food size	8	-2870.3	5756.9	7.4
~ log(Food ration) x Temperature + Temperature x Food size	8	-2870.7	5757.8	8.3
~ log(Food ration) x Temperature + Food size	7	-2875.4	5764.9	15.4
~ log(Food ration) x Food size + Temperature x Food size	8	-2875.7	5767.7	18.2
~ log(Food ration) x Food size + Temperature	7	-2880.3	5774.8	25.3
~ log(Food ration) + Food size x Temperature	7	-2880.8	5775.7	26.2
~ log(Food ration) x Food size	6	-2884.1	5780.4	30.8
~ log(Food ration) + Food size + Temperature	6	-2885.2	5782.6	33.1
~ log(Food ration) + Food size	5	-2889.0	5788.2	38.6
~ Food size x Temperature	6	-2975.1	5962.5	212.9
~ Food size + Temperature	5	-2978.1	5966.3	216.7
~ Food size	4	-2981.9	5971.9	222.3
~ log(Food ration) x Temperature	6	-3099.5	6211.2	461.7
~ log(Food ration) + Temperature	5	-3103.4	6216.9	467.4
~ log(Food ration)	4	-3107.1	6222.2	472.7
~ Temperature	4	-3147.1	6302.2	552.7
~ 1	3	-3150.8	6307.6	558.1

1110

1111 *Table S9: Results of the selected mixed effect model on the maximal oxygen consumption during*
 1112 *feeding (Estimates, 95% confidence intervals and p-values). Estimations of the predictors of all other*
 1113 *fixed effects were based on the estimations of treatment 'warm temperature and small particles'. The*
 1114 *selected model is presented using REML estimation. Food ration was log-transformed before*
 1115 *regression.*

1116

Fixed effects:

<i>Predictors</i>	<i>Estimates</i>	<i>95% CI</i>	<i>p-value</i>
(Intercept)	563.38	525.07 – 601.69	<0.001
log(Food ration)	57.86	46.18 – 69.53	<0.001
Food size [Large]	-154.24	-176.38 – -132.11	<0.001
Temperature [Cool]	-130.42	-183.56 – -77.29	<0.001
log(Food ration) x Food size [Large]	22.10	8.59 – 35.61	0.001
log(Food ration) x Temperature [Cool]	-31.11	-44.62 – -17.60	<0.001
Food size [Large] x Temperature [Cool]	36.14	13.02 – 59.26	0.002

Random Effects:

σ^2	4404.37
$\tau_{00 \text{ Tank}}$	1208.92
ICC	0.22
N_{Tank}	8

Observations	509
Marginal R ² / Conditional R ²	0.650 / 0.726

1117

1118

1119 *Table S10: Results of model selection on the feeding duration (df, logLik, AICc and ΔAICc). The best-*
 1120 *fitting model was selected based on the lowest AICc values (Burnham and Anderson, 2002) following*
 1121 *Zuur et al. 2003. When difference in AICc (ΔAICc) was lower than two between these models, the more*
 1122 *parsimonious model was selected (Burnham and Anderson, 2002). The selected models is represented*
 1123 *in bold. Food ration was second order polynomial transformed for model selection.*

1124

Models	df	logLik	AICc	ΔAICc
~ poly(Food ration) x Temperature + poly(Food ration) x Food size	11	-3283.3	6589.2	0.0
~ poly(Food ration) x Temperature + Temperature x Food size + poly(Food ration) x Food size	12	-3282.5	6589.6	0.4
~ poly(Food ration) x Food size + Temperature	9	-3286.0	6590.4	1.2
~ poly(Food ration) x Food size + Temperature x Food size	10	-3285.2	6591.0	1.7
~ poly(Food ration) x Food size x Temperature	14	-3282.3	6593.5	4.3
~ poly(Food ration) x Food size	8	-3288.7	6593.7	4.5
~ Food size + Temperature	5	-3299.6	6609.3	20.1
~ poly(Food ration) x Temperature + Food size	9	-3295.8	6609.9	20.7
~ Food size x Temperature	6	-3298.9	6610.0	20.8
~ poly(Food ration) x Temperature + Temperature x Food size	10	-3295.0	6610.5	21.3
~ poly(Food ration) + Food size + Temperature	7	-3298.5	6611.3	22.1
~ poly(Food ration) + Food size x Temperature	8	-3297.8	6612.0	22.7
~ Food size	4	-3302.0	6612.2	22.9
~ poly(Food ration) + Food size	6	-3301.0	6614.2	25.0
~ Temperature	4	-3326.4	6661.0	71.8
~ 1	3	-3328.5	6663.1	73.9
~ poly(Food ration) x Temperature	8	-3323.7	6663.7	74.5
~ poly(Food ration) + Temperature	6	-3325.9	6664.1	74.8
~ poly(Food ration)	5	-3328.0	6666.2	77.0

1125

1126

1127

1128

1129

1130

1131

1132 Table S11: Results of the selected mixed effect model on the feeding duration (Estimates, 95%
 1133 confidence intervals and p-values). Estimations of the predictors of all other fixed effects were based
 1134 on the estimations of treatment 'warm temperature and small particles'. The selected model is
 1135 presented using REML estimation. Food ration was second order polynomial transformed before
 1136 regression.

1137

Fixed effects:			
<i>Predictors</i>	<i>Estimates</i>	<i>95% CI</i>	<i>p-value</i>
(Intercept)	906.09	795.90 – 1016.28	<0.001
poly(Food ration, deg = 2) [coef 1]	-133.39	-526.26 – 259.49	0.505
poly(Food ration, deg = 2) [coef 2]	-34.19	-249.79 – 181.40	0.755
Food size [Large]	-448.82	-595.85 – -301.80	<0.001
Temperature [Cool]	-75.92	-139.61 – -12.23	0.020
poly(Food ration, deg = 2) [coef 1] x Food size [Large]	474.35	-69.23 – 1017.92	0.087
poly(Food ration, deg = 2) [coef 2] x Food size [Large]	-82.83	-381.48 – 215.82	0.586
Random Effects:			
σ^2	118832.80		
$\tau_{00 \text{ Tank}}$	0.00		
N_{Tank}	8		
Observations	453		
Marginal R ² / Conditional R ²	0.169 / NA		

1138

1139

1140

1141

1142